Elsevier Editorial System(tm) for ISA Transactions

Manuscript Draft

Manuscript Number: ISATRANS-D-18-00683R2

Title: Deadzone compensation control based on detection of micro flow rate in pilot stage of proportional directional valve

Article Type: Research article

Section/Category: Application

Keywords: Deadzone compensation; pilot operated; proportional directional valve; micro flow rate; deadzone detection; position control.

Corresponding Author: Dr. Junhui Zhang, Ph.D.

Corresponding Author's Institution: State Key Laboratory of Fluid Power and Mechatronic Systems, Zhejiang University

First Author: Zhengyu Lu

Order of Authors: Zhengyu Lu; Junhui Zhang, Ph.D.; Bing Xu; Di Wang; Qi Su; Jinyuan Qian; Min Pan; Geng Yang

Abstract: The pilot operated proportional directional valves (POPDVs) with a flow rate ranging from 100 to 1000 L/min are widely used in electro-hydraulic systems (EHSs). The deadzone of the pilot stage valve and its control compensation could significantly affect the position control performance for the main stage valve that could directly affect dynamics of EHSs. In this paper, it is concluded that micro flow rates exist at the intermediate position of the valve based on the analysis of the continuity equation of the flow in the control chamber of the pilot stage. The micro flow rate is helpful to eliminate the discontinuity and unsmooth domain in the previous inverse deadzone compensation function. An improved deadzone detection method is proposed to calibrate the pilot valve flow characteristics which include the micro flow rate. This new method avoids the threshold selection of the main valve spool displacement which affects the detected deadzone values. Its detection processes are realized based on the pilot flow rate characterized by the speed of the main valve spool and the pilot valve displacement characterized by the solenoid current. The deadzone compensation control strategy based on the improved deadzone detection method is also designed. The experimental results using the steady-state position tracking and sinusoidal position tracking methods are verified. It is concluded that the tracking accuracy of the main valve spool position is effectively improved with this control strategy.

Suggested Reviewers: Ill-Yeong Lee
School of Mechanical Engineering, Pukyong National University
iylee@pknu.ac.kr
Given the reviewer's expertise in this area, he is very suitable to review this article and can give professional comments.

Xiangdong Kong
School of Mechanical Engineering, Yanshan University

xdkong@ysu.edu.cn
Given the reviewer's expertise in this area, he is very suitable to review this article and can give professional comments.

Research Data Related to this Submission
---
There are no linked research data sets for this submission. The following reason is given:
The data that has been used is confidential

# Covering Letter

Date: March 23, 2019.

Dear editor:

We would like to submit the revised manuscript entitled "Deadzone compensation control based on detection of micro flow rate in pilot stage of proportional directional valve", which we wish to be considered for publication in "*ISA Transactions"*.

As it is well know that the pilot operated proportional directional valves are widely used in electro-hydraulic systems (EHSs), the pilot stage deadzone of the pilot operated proportional directional valve and its compensation determine the performance of position control of the main valve directly.

In this paper, we have proposed **an improved deadzone detection method. This method is based on the pilot valve flow characteristics, which includes the micro flow rate of pilot valve. Then, the deadzone compensation control strategy based on the improved the deadzone detection method is designed, and the tracking accuracy of the main valve spool position control is improved effectively.**

In the revision, we have removed the corresponding Reference according to the comments from Deputy Editor-in-Chief.

We notice that the journal, *ISA Transactions aims to be the respected journal of advances in the science and engineering of process measurement and automation.* We would like kindly to point out that **this research just aims to improve the position control accuracy of the pilot operated proportional directional valve by an improved deadzone compensation method**, which would be suitable for areas of this journal.

We promise that the presented work has not been submitted elsewhere for publication, and all the authors listed have approved the manuscript.

Correspondence should be addressed to Junhui Zhang.

Affiliation: State Key Laboratory of Fluid Power and Mechatronic Systems, Zhejiang University

Postal Address: No. 38 Zheda Road, Hangzhou, 310027, China

E-mail Address: bxu@zju.edu.cn

Tel: +86-571-87952505

Fax: +86-571-87952507

Thank you very much for your attention and consideration.

Yours sincerely,

Junhui Zhang

*Title page showing Author Details

# Deadzone compensation control based on detection of micro flow rate in pilot stage of proportional directional valve


## Author names and affiliations

**Zhengyu Lu**
Affiliation: The State Key Laboratory of Fluid Power and Mechatronic Systems, Zhejiang University
Postal Address: No.38 Zheda Road, Hangzhou, 310027, China
E-mail Address: luzhenyu@zju.edu.cn

**Junhui Zhang**
Affiliation: The State Key Laboratory of Fluid Power and Mechatronic Systems, Zhejiang University
Postal Address: No.38 Zheda Road, Hangzhou, 310027, China
E-mail Address: benzjh@zju.edu.cn
Tel: +86-571-87952505
Fax: +86-571-87952507

**Bing Xu**
Affiliation: The State Key Laboratory of Fluid Power and Mechatronic Systems, Zhejiang University
Postal Address: No.38 Zheda Road, Hangzhou, 310027, China
E-mail Address: bxu@zju.edu.cn

**Di Wang**
Affiliation: The State Key Laboratory of Fluid Power and Mechatronic Systems, Zhejiang University
Postal Address: No.38 Zheda Road, Hangzhou, 310027, China
E-mail Address: di_wang@zju.edu.cn

**Qi Su**
Affiliation: The State Key Laboratory of Fluid Power and Mechatronic Systems, Zhejiang University
Postal Address: No.38 Zheda Road, Hangzhou, 310027, China
E-mail Address: 06jxlsq@zju.edu.cn

**Jinyuan Qian**
Affiliation: Institute of Prcocess Equipment, College of Energy Engineering, Zhejiang University
Postal Address: No.38 Zheda Road, Hangzhou, 310027, China
E-mail Address: qianjy@zju.edu.cn

**Geng Yang**
Affiliation: The State Key Laboratory of Fluid Power and Mechatronic Systems, Zhejiang University
Postal Address: No.38 Zheda Road, Hangzhou, 310027, China
E-mail Address: yanggeng@zju.edu.cn

**Min Pan**

Affiliation: The Centre for Power Transmission and Motion Control, University of Bath
Postal Address: Claverton Down, Bath, North East Somerset BA2 7AY, United Kingdom
E-mail Address: M.Pan@bath.ac.uk

## Corresponding author

**Junhui Zhang**
Affiliation: The State Key Laboratory of Fluid Power and Mechatronic Systems, Zhejiang University
Postal Address: No.38 Zheda Road, Hangzhou, 310027, China
E-mail Address: benzjh@zju.edu.cn
Tel: +86-571-87952505
Fax: +86-571-87952507

# Response to Editor

Dear Editor,

We really appreciate the constructive comments expressed by the Editor-in-Chief, Technical Editor, and reviewers about our work. According to the comments from Deputy Editor-in-Chief we have removed the Reference *"[21] J. Yu, P. Shi, W. Dong, C. Lin. Adaptive Fuzzy Control of Nonlinear Systems With Unknown Dead Zones Based on Command Filtering. IEEE Trans. Fuzzy Syst. 2018; 26(1):46-55. [22] J. Yu, P. Shi, W. Dong, C. Lin. Command Filtering-Based Fuzzy Control for Nonlinear Systems With Saturation Input, IEEE T. Cybern. 2017;47(9):2472-2479."* in the revised manuscript. And the corresponding reference marks have been modified.

The specific responses to the comments of the reviewers are listed below. The comments are marked in violet, and the responses are marked in black.

Thank you very much!

# Response to Reviewers

## Response to Reviewer #1

**I satisfied authors' replies for all issues.**

The authors are grateful to the reviewer for his/her approval of the previous revised manuscript.

## Response to Reviewer #2

**It can be accepted.**

Thank the reviewer for his/her approval of our work.

## Response to Reviewer #4

**I would like to thank the authors for addressing all my comments.**

Thanks a lot for the reviewer's comments and his/her approval.

# Graphical abstracts

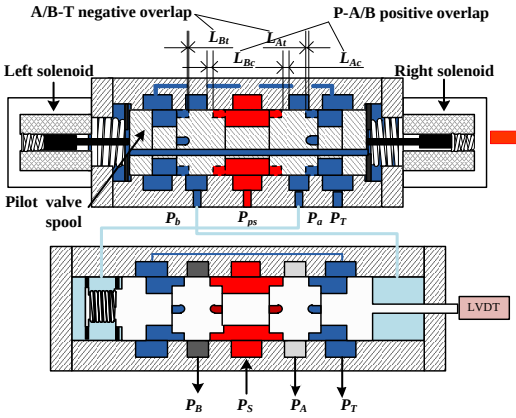


The overlaps of the proportional directional valve

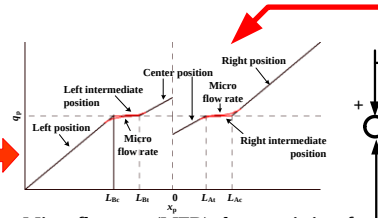


Micro flow rate (MFR) characteristics of the pilot valve

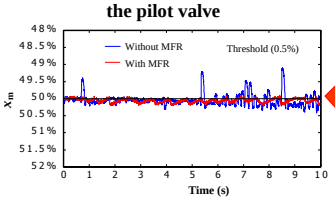


Experimental results of deadzone compensation control

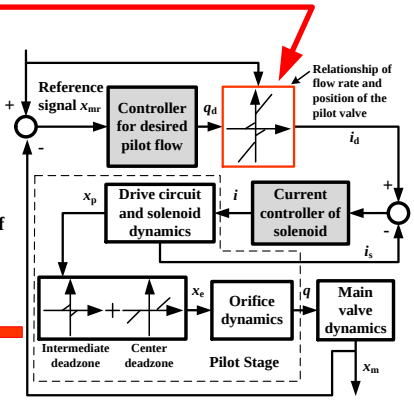


The closed-loop position control of the main valve

# Highlights

(1) An improved deadzone detection method is proposed.

(2) The micro flow rate in the pilot stage is detected.

(3) The deadzone compensation control strategy with calibrated flow rate characteristic of the pilot valve is proposed.

(4) The accuracy of the position control of the main valve is improved.

# Deadzone compensation control based on detection of micro flow rate in pilot stage of proportional directional valve

**Abstract:**

The pilot operated proportional directional valves (POPDVs) with a flow rate ranging from 100 to 1000 L/min are widely used in electro-hydraulic systems (EHSs). The deadzone of the pilot stage valve and its control compensation could significantly affect the position control performance for the main stage valve that could directly affect dynamics of EHSs. In this paper, it is concluded that micro flow rates exist at the intermediate position of the valve based on the analysis of the continuity equation of the flow in the control chamber of the pilot stage. The micro flow rate is helpful to eliminate the discontinuity and unsmooth domain in the previous inverse deadzone compensation function. An improved deadzone detection method is proposed to calibrate the pilot valve flow characteristics which include the micro flow rate. This new method avoids the threshold selection of the main valve spool displacement which affects the detected deadzone values. Its detection processes are realized based on the pilot flow rate characterized by the speed of the main valve spool and the pilot valve displacement characterized by the solenoid current. The deadzone compensation control strategy based on the improved deadzone detection method is also designed. The experimental results using the steady-state position tracking and sinusoidal position tracking methods are verified. It is concluded that the tracking accuracy of the main valve spool position is effectively improved with this control strategy.

**Keywords:**

Deadzone compensation; pilot operated; proportional directional valve; micro flow rate; deadzone detection; position control.

# 1 Introduction

The pilot operated proportional directional valves (POPDVs) with a flow rate ranging from 100 to 1000 L/min are widely used in electro-hydraulic systems (EHSs) [1]. As a key component, the POPDV could significantly affect the control performance of EHSs. For example, the dimensional accuracy and consistency of injection molding products are directly controlled by the dynamic characteristics and control accuracy of a POPDV [2]. Therefore, many researches focus on improving the control characteristics of POPDV.

The pilot stage and the main stage of a POPDV constitute a typical position closed-loop valve-controlled cylinder system as shown in Fig. 1 [3]. In this system, the input signals are the currents of two solenoids in the pilot stage, and the output signal is the main valve spool displacement, which is measured by a Linear Variable Differential Transformer (LVDT) displacement sensor and feed back to the control unit. The control strategy plays a key role for the dynamic characteristics and control accuracy of a POPDV. In order to improve the control performance of hydraulic valves, researchers have proposed various control methods. J. B. Gamble et al. adopted sliding mode control, and optimized the optimization of the sliding surface under the restriction of the jerk of spool. The response speed of the direct acting proportional servo valve has been improved [4]. Jin-hui Fang et al., introduced the integral action and speed feedback to improve the steady-state control accuracy and dynamic tracking performance of the proportional servo valve based on the jerk-constrained optimization sliding mode control [5]. Christoph Krimpmann et al. proposed two-order nonlinear sliding mode control method, which adopted active pole optimization method, the automatic tuning control parameters and the parameters of synovial pole [6], to further improve the control performance of direct acting proportional servo valve [7]. These control methods require accurate pilot valve spool position, and are not suitable for the POPDV without position sensor in the pilot stage.

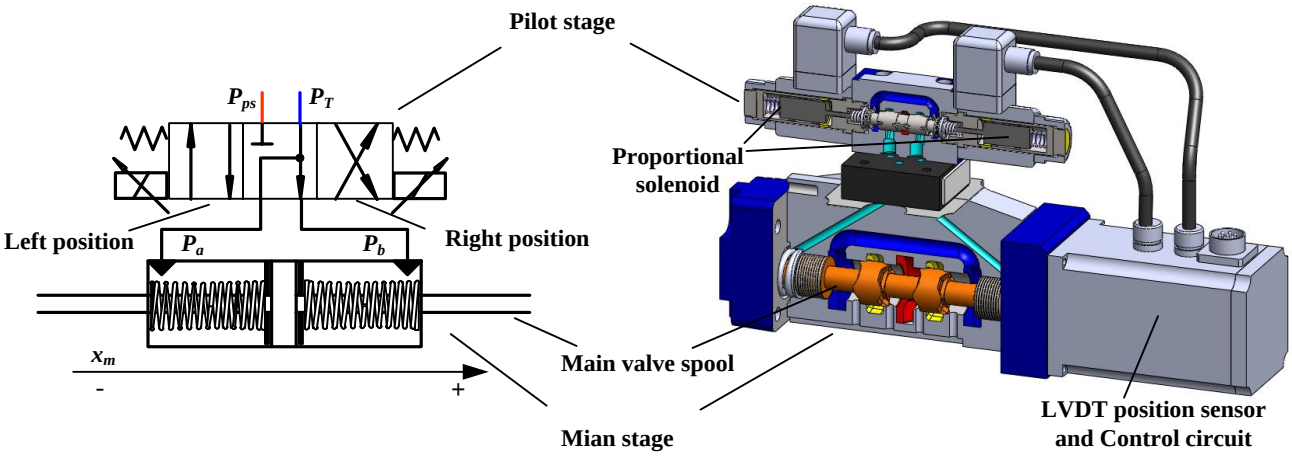


**Fig. 1. The pilot operated directional valve and its schematic as a valve-controlled cylinder system.**

To a certain extent, the driving force of the pilot valve spool is proportional to the solenoid current, and the driving force of the main valve spool is proportional to the pressure in the control chambers. Therefore, the position control strategy design for the main valve spool focuses on the flow rate control in the pilot stage. However, in order to reduce manufacturing costs and sensitivity to contamination of oil, there are positive overlaps between the spool and the housing for the pilot stage [8, 9], resulting in the deadzones between the pilot valve spool displacement and the valve opening. The deadzones could improve the anti-disturbance capability of a POPDV, but they have significant adverse effects on the flow rate characteristics of the pilot stage. The deadzones also influence the dynamic characteristics and control accuracy of POPDVs. Therefore, accurate deadzone compensation is an important step in the control strategy design of POPDVs [10-12].

The most common method of deadzone compensation is using a constant inverse compensation function to counteract or compensate the influence of deadzone, which is effective only if the deadzones are fixed and known in advance [10-12]. However, the deadzones are not fixed but could be influenced by overlap, temperature, and clearance for a POPDV.

Therefore, for the deadzone with unknown parameters, the adaptive methods [13-16] are proposed to obtain the deadzone information online for compensation control. For the deadzone with time-varying characteristics, the neural network [17-20] methods were employed to adjust the deadzone inverse compensation parameters.

These deadzone compensation methods could improve the dynamic characteristics and control accuracy of a POPDV evidently, but the online detection of varying deadzones in these researches relied on extra sensors including a LVDT displacement sensor in the pilot stage, which is impractical for the POPDVs as shown in Fig.1 due to the cost restriction. In addition, these methods considered only the compensation of the center deadzone. However, it was noted that the deadzones of the pilot valve were a cascade model with a center deadzone and an intermediate deadzone according to the flow characteristics of the pilot valve [12, 21]. The application of the cascade deadzone model in compensation control instead of the center deadzone model effectively improved the performance of a POPDV. The compensation method reduced the tracking error of the main valve spool position and the tracking lag at the direction changing moment of main valve spool motion as shown in Fig. 2. However, two aspects for the cascade deadzone model can be modified to further improve the control accuracy of the main valve. Firstly, due to the gap and leakage of the pilot valve, there is micro flow rate when the pilot valve spool has positive overlaps. This flow rate is simplified as zero in the cascade deadzone model. This simplification introduces discontinuity and unsmooth domain in the control law, and influences the position control accuracy of the main valve spool. Secondly, in the deadzone detection process, the deadzone is measured by the motion state of the main valve spool, and it needs to select a threshold of the main valve spool displacement to judge the spool motion, so as to calibrate the deadzone value. The threshold directly affects the detected deadzone values, thus affecting the position control accuracy of the main valve spool. These two aspects will be discussed in detail in the following part.

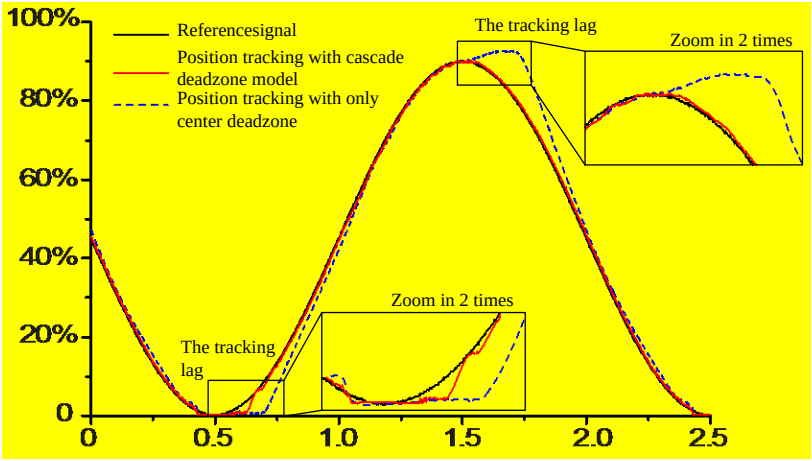


**Fig. 2. Position tracking performances with only center deadzone compensation and with cascade deadzone model.**

In this paper, an improved deadzone compensation control method is proposed, which is based on the flow characteristics of the pilot valve considering the micro flow rate. The deadzone model is modified from a hard state to a soft state by this method [22]. Applying this deadzone model to the inverse deadzone compensation control could further improve the control accuracy of the main valve. The paper is organized as follows. The cascade deadzone model of the pilot valve is reviewed, and an additional analysis of the deadzone compensation method is carried out based on the continuity equation of the flow in the control chamber of pilot stage. The improved detection method of the deadzones is introduced in detail, and the calibration results containing the micro flow characteristics are analyzed in the third section, followed by the control strategy of the deadzone compensation. In the fifth section, the pilot stage deadzone model considering the micro flow rate of the pilot valve is applied to the position control of the main valve spool, and is verified by experimental data. Finally, some necessary summaries are concluded.

# 2 Deadzone compensation method based on cascade deadzone model

## 2.1 Cascade deadzone model and micro flow rate of the pilot stage

Ports A, B of the pilot valve have positive and negative overlaps $L_{Ac}$, $L_{At}$, $L_{Bc}$, $L_{Bt}$, as shown in Fig. 3 (a). According to

the relative position between the pilot valve displacement $x_P$ and the overlap, the pilot valve has five working positions. As shown in Fig. 3 (b), they are namely, left position, left intermediate position, center position, right intermediate position, and right position. The flow rate characteristics of the five positions are shown in Fig. 4. When the pilot valve is in the left or right position, the main valve spool is driven by the fluid through the pilot valve port, which can be called driving flow. The pilot valve has a deadzone when it is in the left or right intermediate position. When the pilot valve is in the center position and the main valve moves to the right or left position, the pressure of the pilot control chamber is balanced with the spring force of the main stage. When the main valve moves back to the center position, there will be flow rate through the pilot valve port due to the pressure of the pilot control chamber, which is called damping flow. This relationship between the pilot valve position and the flow rate is a cascade deadzone model consisting of the intermediate deadzone and center deadzone[12, 21].

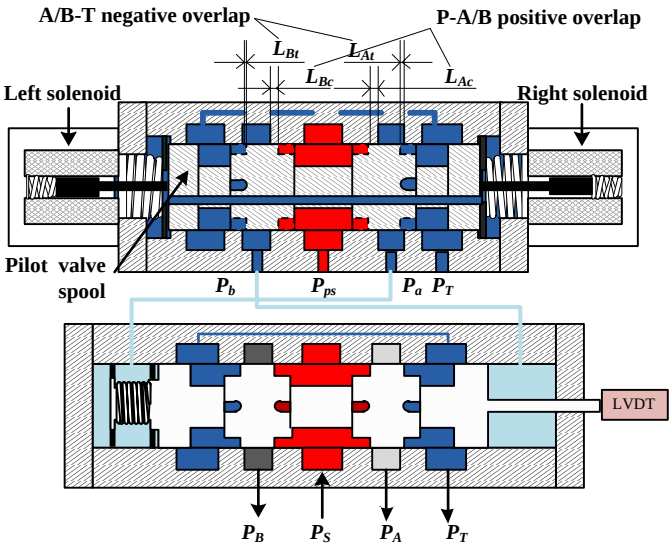


(a) The structure of pilot operated proportional directional valve with overlaps

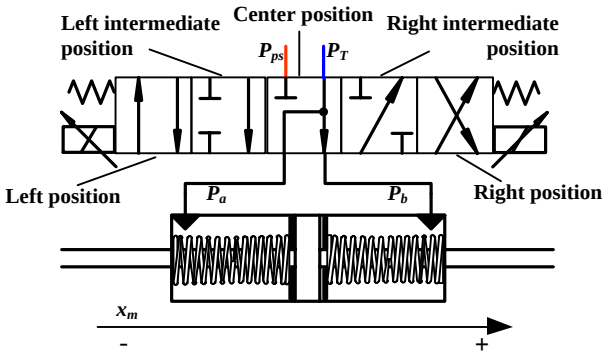


(b) The schematic of the valve with detailed pilot valve working positions

**Fig. 3. The structure and schematic of the pilot operated directional valve.**

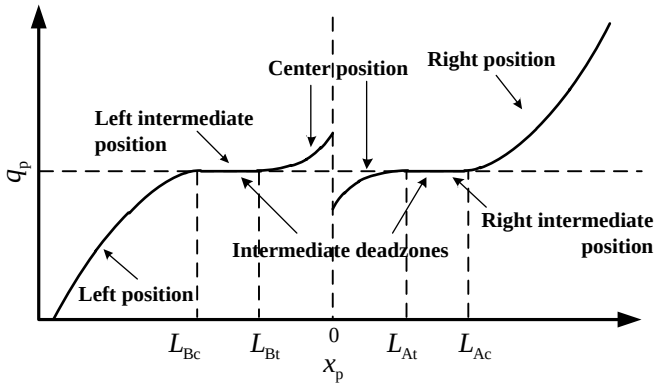


**Fig. 4. Flow rate characteristics of the pilot valve.**

In the previous research, it is shown that the intermediate deadzones of the pilot valve are not directly equal to the overlaps of A and B ports, due to the leakage of the gap between the pilot valve spool and housing. As shown in Fig. 5, take port A of the pilot valve as an example. When the pilot valve spool displacement is between $L_{Ac}$ and $L_{At}$, as shown in Fig. 5 (b), the flow rate $q_{pa}$, which is from the pilot port to the pilot control chamber, is laminar flow through annular clearance[1].

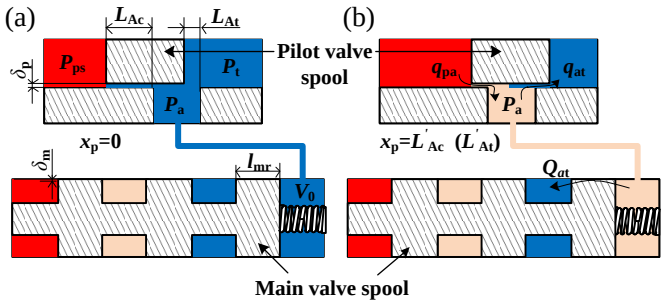


**Fig. 5. The leakages cause by the clearance of the valve spool.**

$$q_{pa} = \frac{\pi d_p \delta_p^{\ 3}}{12\mu} \cdot \frac{p_{ps} - p_a}{L_{Ac} - x_p} \tag{1}$$

where $d_P$ is the diameter of pilot valve spool; $\delta_p$ is the clearance between the pilot valve spool and housing; $\mu$ is oil viscosity; $p_{ps}$ is the supply pressure of the pilot valve, which is 3MPa; $p_a$ is pressure in the pilot control chamber A.

The leakage flow rate from the pilot control chamber to the pilot valve return port is

$$q_{at} = \frac{\pi d_p \delta_p^{\ 3}}{12\mu} \cdot \frac{p_a}{x_p - L_{At}} . \tag{2}$$

The leakage flow rate from the pilot control chamber to the main valve return port is

$$Q_{at} = \frac{\pi d_m \delta_m^{\ 3}}{12\mu} \cdot \frac{p_a}{l_{mr}} , \tag{3}$$

where the $d_m$ is the diameter of main valve spool; $\delta_m$ is the gap between the main valve spool and housing; $l_{mr}$ is the gap length, which changes with movement of the main valve spool.

When the pilot valve is at the intermediate position, the flow rate of the pilot control chamber satisfies

$$q_{pa} - q_{at} - Q_{at} - A_v \dot{x}_m - \frac{\dot{p}_a (V_0 + A_v x_m)}{\beta_e} = 0 , \tag{4}$$

where $A_v$ is cross-sectional area of the main valve spool; $x_m$ is the displacement of main valve spool; and $V_0$ is the initial volume of pilot control chamber; $\beta_e$ is the oil bulk modulus.

In this case, the main valve spool is in a static state. According to Newton's second law, the force equilibrium equation is

$$M\ddot{x}_{\mathrm{m}} = A_{\mathrm{v}}(p_{\mathrm{a}} - p_{\mathrm{b}}) - F_{\mathrm{mk0}} - F_{\mathrm{mf}}\,\mathrm{sgn}(\dot{x}_{\mathrm{m}}), \tag{5}$$

where $M$ is the mass of the main valve spool; $F_{\mathrm{mk0}}$ is the initial preload spring force of the main stage; $F_{\mathrm{mf}}$ is the viscous friction force of the main valve; $p_{\mathrm{b}}$ is the pressure of the pilot control chamber B. According to this equilibrium equation, the pressure of the pilot control chamber can be calculated.

When the pilot valve moves to the upper limit of the intermediate deadzone, i.e. $x_{\mathrm{p}}=L'_{\mathrm{Ac}}$, the main valve begins to move from the static state that $x_{\mathrm{m}}=0$. According to the force equilibrium equation of main valve spool, the pressure and the flow rate of the pilot control chamber satisfy

$$\begin{cases} p_{\mathrm{a}} = \dfrac{4\left(F_{\mathrm{mk0}} + F_{\mathrm{mf}}\right)}{\pi d_{\mathrm{m}}^{2}} \\ \dfrac{\pi d_{\mathrm{p}} \delta_{\mathrm{p}}^{3}}{12\mu} \cdot \left( \dfrac{p_{\mathrm{s}} - p_{\mathrm{a}}}{L_{\mathrm{Ac}} - L'_{\mathrm{Ac}}} - \dfrac{p_{\mathrm{a}}}{L'_{\mathrm{Ac}} - L_{\mathrm{At}}} \right) = \dfrac{\pi d_{m} \delta_{\mathrm{m}}^{3}}{12\mu} \dfrac{p_{\mathrm{a}}}{l_{\mathrm{mr}}} + \dfrac{p_{\mathrm{a}}}{t} \cdot \dfrac{V_0}{\beta_{\mathrm{e}}} \end{cases}, \tag{6}$$

where the pressure gradient of the control chamber $p_{\mathrm{a}}$ is about $p_{\mathrm{a}}/t$. Solving the above equations, we can get the actual upper limit $L'_{\mathrm{Ac}}$ of the intermediate deadzone.

When the main valve spool is in a certain position that $x_{\mathrm{m}}=X_{\mathrm{m}}$ and the pilot spool moves to the lower limit of the intermediate deadzone that $x_{\mathrm{p}}=L'_{\mathrm{At}}$, the main valve begins to move back to the center position. In this case, the pressure and the flow rate of the pilot control chamber satisfy

$$\begin{cases} p_{\mathrm{a}} = \dfrac{4\left(F_{\mathrm{mk0}} - F_{\mathrm{mf}} + k_{\mathrm{m}} X_{\mathrm{m}}\right)}{\pi d_{\mathrm{m}}^{2}} \\ \dfrac{\pi d_{\mathrm{p}} \delta_{\mathrm{p}}^{3}}{12\mu} \cdot \left( \dfrac{p_{\mathrm{s}} - p_{\mathrm{a}}}{L_{\mathrm{Ac}} - L'_{\mathrm{At}}} - \dfrac{p_{\mathrm{a}}}{L'_{\mathrm{At}} - L_{\mathrm{At}}} \right) = \dfrac{\pi d_{m} \delta_{\mathrm{m}}^{3}}{12\mu} \dfrac{p_{\mathrm{a}}}{l_{\mathrm{mr}} - X_{\mathrm{m}}} + \dfrac{p_{\mathrm{a}}}{t} \cdot \dfrac{(V_0 + A_{\mathrm{v}} X_{\mathrm{m}})}{\beta_{\mathrm{e}}} \end{cases}. \tag{7}$$

The actual lower limit of the intermediate deadzone can be obtained by Eq. (7). The actual deadzone values calculated by Eqs.(6)-(7) are not consistent with the overlap values due to the gap leakage, which means that there is micro flow rate due to the difference between the actual deadzone and overlap, as shown in Fig. 6.

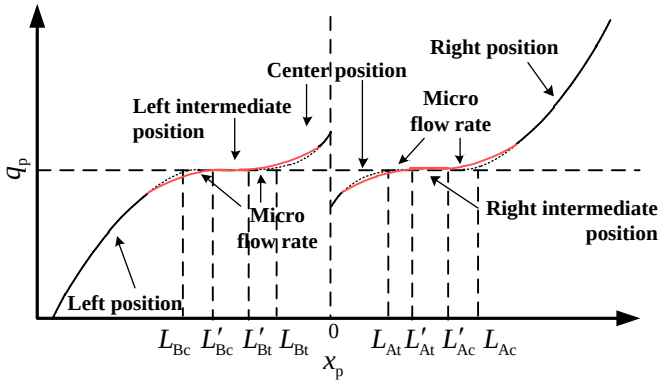


**Fig. 6. Micro flow rate at the intermediate position.**

## 2.2 Analysis of previous deadzone compensation method

In the detection of the deadzone parameters as mentioned in the previous research [12, 21] , we assumed that the current of the proportional solenoid has a linear relationship with the magnetic force acting on the pilot spool within the stroke of deadzone at slow speed. Then, even without displacement sensor in the pilot stage of the proportional valve, the current of the solenoid $I_{\mathrm{p}}$ can be used to characterize the pilot valve displacement, as shown in Eq. (8) [21].

$$I_{\mathrm{p}} = \frac{k_{\mathrm{pk}} x_{\mathrm{p}}}{k_{\mathrm{I}}} \tag{8}$$

where $k_{\mathrm{pk}}$ is the stiffness of the pilot stage spring; $k_{\mathrm{I}}$ is the gain coefficient of the solenoid current force. Then the

deadzone parameters $L_{Ac}$, $L_{At}$, $L_{Bc}$, $L_{Bt}$, can be detected and characterized as the current of the solenoid $I_{Ac}$, $I_{At}$, $I_{Bc}$, $I_{Bt}$. The detection processes are shown in Fig. 7, and it is necessary to set a threshold of the main valve spool displacement to monitor the motion of the main valve spool.

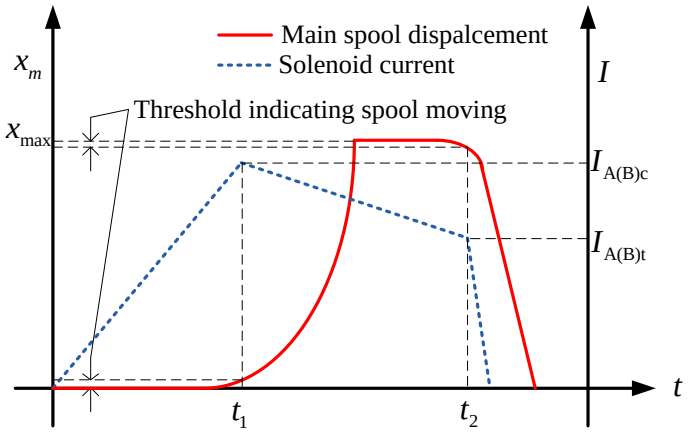


**Fig. 7. Detection of deadzone parameters characterized as the solenoid current.**

Then with the deadzone parameters characterized as the solenoid current, the inverse of the cascade deadzone model is used to compensate the cascade deadzones, which can be described by

$$I_d = CDZI\left(q_{pd}\right) = \begin{cases} \dfrac{k_{pk} q_{pd}}{k_i \omega_a C_d \sqrt{2(p_{ps} - p_a)/\rho}} + I_{Ac} & \text{if } x_m > 0, q_{pd} > 0 \\ \dfrac{I_{Ac} + I_{At}}{2} & \text{if } x_m > 0, q_{pd} = 0 \\ \dfrac{k_{pk} q_{pd}}{k_i \omega_a C_d \sqrt{2 p_a / \rho}} + I_{At} & \text{if } x_m > 0, q_{pd} < 0 \\ 0 & \text{if } x_m = 0 \\ \dfrac{k_{pk} q_{pd}}{k_i \omega_b C_d \sqrt{2 p_b / \rho}} - I_{Bt} & \text{if } x_m < 0, q_{pd} > 0 \\ -\dfrac{I_{Bc} + I_{Bt}}{2} & \text{if } x_m < 0, q_{pd} = 0 \\ \dfrac{k_{pk} q_{pd}}{k_i \omega_b C_d \sqrt{2(p_{ps} - p_b)/\rho}} - I_{Bc} & \text{if } x_m < 0, q_{pd} < 0 \end{cases}, \quad (9)$$

where $C_d$ is the flow coefficient of the pilot valve ports; $\omega_a$, $\omega_b$ are the equivalent circumference of the pilot valve ports; $q_{pd}$ is the desired flow rate calculated by the main valve position controller which is a PID controller in the previous research. This inverse deadzone compensation method ignores the micro flow rate in the intermediate deadzone. And this simplification leads to the discontinuity and unsmooth domain of the desired solenoid current in the neighborhood of $q_{pd}$=0 as shown in Eq. (9), which influences the further improvement of tracking accuracy of the position control of the main valve spool.

What's more, the threshold to monitor the motion of the main valve spool in the deadzone detection also affects the detected deadzone values $L'_{Ac}$, $L'_{At}$ $L'_{Bc}$ $L'_{Bt}$, which has a direct effect on the deadzone compensation. That is, when the pilot valve spool displacement slowly increases or decreases during a time period of $t_c$, the main valve spool moving across $C_e$% of the full stroke is selected as the threshold to determine deadzone values of the pilot valve. In this detection process, when the main valve spool displacement is greater or smaller than this threshold, the pilot valve displacement at this moment is calibrated as the upper or lower limit value of the intermediate deadzone. Thus the detected deadzone values satisfy the following Eqs. (10), (11) corrected from Eqs. (6), (7) in practical application. Eqs. (10), (11) contain the additional flow rate during the movement of main valve spool.

$$\begin{cases} p_{\mathrm{a}} = \dfrac{4\left(F_{\mathrm{mk0}} + F_{\mathrm{mf}}\right)}{\pi d_{\mathrm{m}}^{2}} \\ \dfrac{\pi d_{\mathrm{p}} \delta_{\mathrm{p}}^{3}}{12\mu} \cdot \left( \dfrac{p_{\mathrm{s}} - p_{\mathrm{a}}}{L_{\mathrm{Ac}} - L'_{\mathrm{Ac}}} - \dfrac{p_{\mathrm{a}}}{L'_{\mathrm{Ac}} - L_{\mathrm{At}}} \right) = \dfrac{\pi d_{m} \delta_{\mathrm{m}}^{3}}{12\mu} \dfrac{p_{\mathrm{a}}}{l_{\mathrm{mr}}} + \dfrac{p_{\mathrm{a}}}{t} \cdot \dfrac{V_0}{\beta_{\mathrm{e}}} + A_{\mathrm{v}} \cdot \dfrac{C_{\mathrm{e}} x_{\mathrm{ml}}}{t_{\mathrm{c}}} \end{cases} \tag{10}$$

$$\begin{cases} p_{\mathrm{a}} = \dfrac{4\left(F_{\mathrm{mk0}} - F_{\mathrm{mf}} + k_{\mathrm{m}} X_{\mathrm{m}}\right)}{\pi d_{\mathrm{m}}^{2}} \\ \dfrac{\pi d_{\mathrm{p}} \delta_{\mathrm{p}}^{3}}{12\mu} \cdot \left( \dfrac{p_{\mathrm{s}} - p_{\mathrm{a}}}{L_{\mathrm{Ac}} - L'_{\mathrm{At}}} - \dfrac{p_{\mathrm{a}}}{L'_{\mathrm{At}} - L_{\mathrm{At}}} \right) = \dfrac{\pi d_{m} \delta_{\mathrm{m}}^{3}}{12\mu} \dfrac{p_{\mathrm{a}}}{l_{\mathrm{mr}} - X_{\mathrm{m}}} + \dfrac{p_{\mathrm{a}}}{t} \cdot \dfrac{(V_0 + A_{\mathrm{v}} X_{\mathrm{m}})}{\beta_{\mathrm{e}}} - A_{\mathrm{v}} \cdot \dfrac{C_{\mathrm{e}} x_{\mathrm{ml}}}{t_{\mathrm{c}}} \end{cases} \tag{11}$$

The parameter values in Table 1 are substituted into (10), (11) to calculate the detected deadzone values. The results are shown in Table 2.

**Table 1 Parameters for deadzone calculation**

| Prameters | Value | Prameters | Value |
|---|---|---|---|
| $V_0$ | 17000mm$^3$ | $d_{\mathrm{m}}$ | 27mm |
| $\delta_{\mathrm{p}}$ | 10μm | $d_{\mathrm{p}}$ | 12mm |
| $l_{\mathrm{mr}}$ | 10mm | $K_{\mathrm{m}}$ | 65N/mm |
| $\beta_{\mathrm{e}}$ | 1200Mpa | $X_{\mathrm{m}}$ | 0.05mm |
| $p_{\mathrm{ps}}$ | 3Mpa | $t$ | 0.2s |
| $\delta_{\mathrm{m}}$ | 2μm | $t_{\mathrm{c}}$ | 0.2s |
| $F_{\mathrm{mk0}}$ | 125N | $F_{\mathrm{mf}}$ | 25N |
| $\mu$ | 0.041Ns/m$^2$ | $A_{\mathrm{v}}$ | 5.72cm$^2$ |
| $L_{\mathrm{Ac}}$ | 1.1mm | $L_{\mathrm{At}}$ | 0.9mm |
| $C_{\mathrm{e}}$ | 0.02; 0.05; 0.1; | $x_{\mathrm{ml}}$ | 5mm |

**Table 2 The values of actual deadzones and detection deadzones**

| Condition | $L'_{\mathrm{Ac}}$ | $L'_{\mathrm{At}}$ |
|---|---|---|
| Real Value | 0.917mm | 0.912mm |
| Calibration Value $C_{\mathrm{e}}$=2% | 0.923mm | 0.910mm |
| Calibration Value $C_{\mathrm{e}}$=5% | 0.937mm | 0.907mm |
| Calibration Value $C_{\mathrm{e}}$=10% | 0.978mm | 0.905mm |

It can be seen that the length ($L'_{\mathrm{Ac}}$-$L'_{\mathrm{At}}$) of the detected intermediate deadzone is widened as the threshold increment accordingly. As the detected deadzone values varying with the threshold, it is necessary to select an appropriate threshold value to get appropriate detected deadzone values empirically for better performance of compensation control.

In conclusion, the previous inverse deadzone compensation function contains discontinuity and unsmooth domain in the neighbourhood of $q_{\mathrm{d}}$=0, and the threshold of the main valve spool displacement affects the detected deadzone values. These two aspects may hinder the further improvement of the control performance.

## 3 Improved deadzone detection method considering micro flow rate at the intermediate position

It is a practical and effective way to directly use the flow characteristics of the pilot valve, which include the micro flow rate at the intermediate position, to improve the control performance of the main valve. It can eliminate the discontinuity and unsmooth domain in the previous inverse deadzone compensation function, and avoid threshold selection

of the main valve spool displacement affecting the detected deadzone values. The improved deadzone detection method is proposed in this section.

Since the inherent frequency of main valve is far quicker than that of the pilot valve, the dynamic characteristics of the main stage can be simplified. All flow rate of the pilot stage in addition to leakage is utilized to drive the main valve spool [23]. Therefore, the flow characteristics of the pilot stage can be expressed by the speed of the main valve spool $v_m$, which is shown in Eq. (12).

$$q_p = v_m A_v + q_{leak} \tag{12}$$

Based on the pilot valve displacement characterized by current and the pilot valve flow rate characterized by the speed of the main valve spool, the improved deadzone detection method is mainly divided into the following six steps, as shown in Fig. 8. The whole detection processes can be realized in the digital controller, and the processes are described as follows.

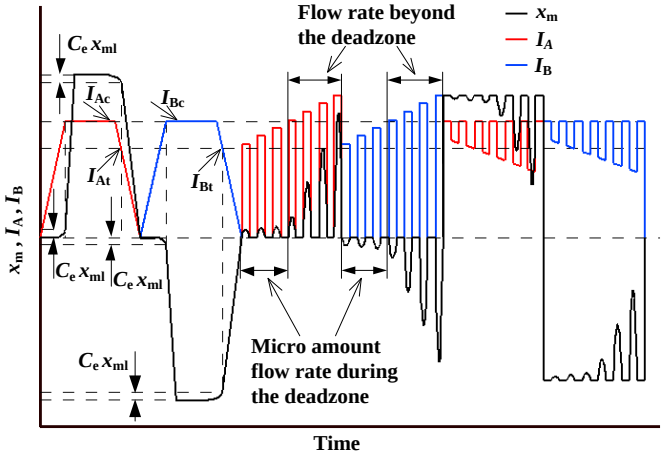


**Fig. 8. Deadzones and micro flow rate detection processes of the pilot valve.**

1) Set the main valve spool at $x_m$=0, and increase the solenoid A current slowly. Then detect the movement of the main valve spool. When the main valve spool displacement is greater than the threshold value $C_e$, record the current of the solenoid A as $I_{Ac}$. Control the main valve spool displacement to be in the $x_m$=$X_m$ position, and let the current of the solenoid A decrease slowly. Then detect the movement of the main valve spool. When the main valve spool movement is less than the threshold $C_e$, record the current of the solenoid A as $I_{At}$.

2) Set the main valve spool at $x_m$=0, and increase the solenoid B current slowly. Then detect the movement of the main valve spool. When the main valve spool displacement is greater than the threshold value $C_e$, record the solenoid current B as $I_{Bc}$. Control the main valve spool displacement to be in the $x_m$=-$X_m$ position, and let the current of the solenoid B decrease slowly. Then detect the movement of the main valve spool. When the main valve spool movement is less than the threshold $C_e$, record the solenoid current B as $I_{Bt}$.

Through the above two steps, the deadzone values characterized by the current are initially calibrated [12]. Then the micro flow rate in the deadzone can be detected as described below.

3) Set the main valve spool at $x_m$=0, and increase the solenoid A current $I_A$ starting from $I_{At}$ with a certain increment in a calibrating step until the current value is greater than the upper limit of the solenoid. In the case of every fixed current, sample the movement of the main valve spool and the time that it spends. The division of the displacement increment and the time can represent the main valve spool speed $v_m$, which is used to calibrate the flow rate of the pilot valve under a certain pilot valve spool displacement characterized by the fixed current. According to this similar method, the driving flow characteristic of the pilot valve port A can be calibrated as $I_A$=$f_{A1}$($v_m$).

4) Through the similar method as step 3, the driving flow characteristic of the pilot valve port B can be calibrated as $I_B$=$f_{B1}$($v_m$).

5) Set the main valve spool at $x_m$=$X_m$, and decrease the solenoid A current $I_A$ starting from $I_{Ac}$ with a certain decrement in a calibrating step until the current value is zero. In the case of every fixed current, sample the movement of the main

valve spool and the time that it spends. The division of the displacement increment and the time can represent the main valve spool valve speed $v_m$, which is used to calibrate the flow rate of the pilot valve under a certain pilot valve spool displacement characterized by the fixed current. According to this similar method, the damping flow characteristic of the pilot valve port A can be calibrated as $I_A=f_{A2}(v_m)$.

6) Using the similar method as step 5, the damping flow characteristic of the pilot valve port B can be calibrated as $I_B=f_{B2}(v_m)$.

It should be pointed out that the change of the main valve spool displacement directly affects the pressure of the pilot control chamber, and has a great influence on the damping flow characteristics of the pilot stage, as shown in Eq. (5). For the different main valve spool displacement $x_m$, the damping flow characteristics of the pilot stage can be corrected by

$$I_{A(B)} = f_{A(B)2}\left(v_m \sqrt{\left|\frac{X_m}{x_m}\right|}\right). \tag{13}$$

Through the above steps, the flow characteristics of the pilot valve which contain the micro flow rate at the intermediate position can be detected. It is worth noting that, the threshold of the main valve spool displacement is used in the initial two steps, but it doesn't need an optimal selection. In fact, it only needs to be greater than the amplitude of the steady-state noise of the main valve displacement sensor.

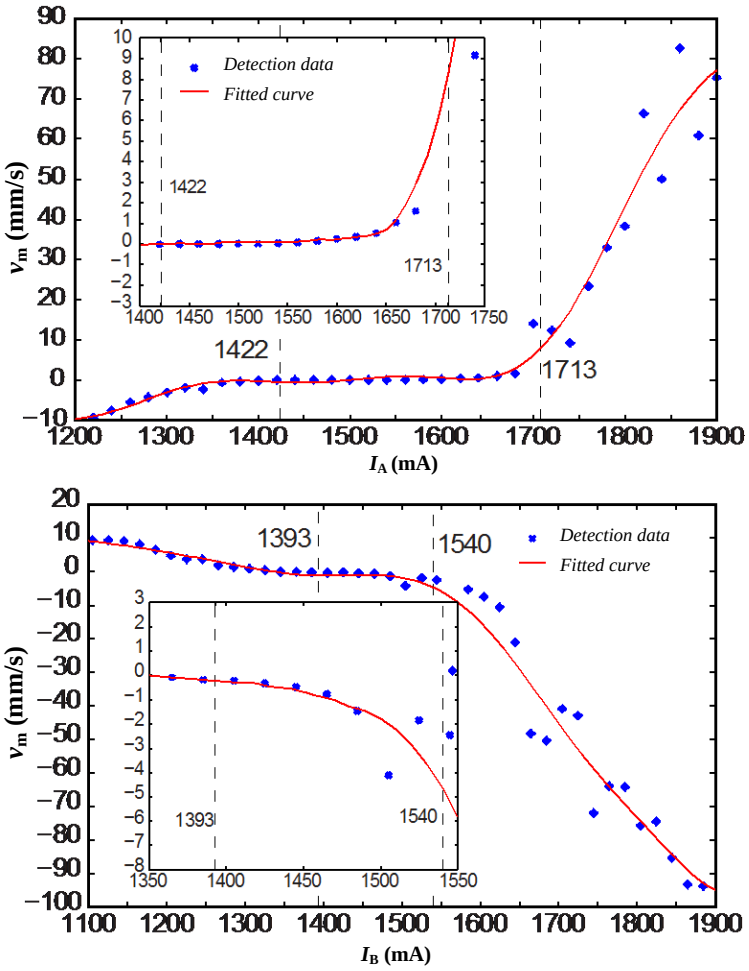


**Fig. 9. Results of flow rate detection.**

The experimental detection results in the case of $X_m$ being 10% stroke (100% ~ 5mm) of the main valve are shown in Fig. 9. The detected deadzone values in the experiment are $I_{Ac}$=1713mA; $I_{At}$=1422mA; $I_{Bc}$=1540mA; $I_{Bt}$=1393mA, which are calibrated in the case of 0.5% threshold and $X_m$ at 90% stroke. According to Fig. 9, the driving flow rate is higher than the damping flow rate. The flow rate characteristics in the detection intermediate position are not zero, but it is far less than the flow rate when the main valve moves out of the deadzone, and so-called micro flow rate.

# 4 Deadzone compensation control strategy with calibrated flow rate characteristic of the pilot valve

Since the inherent frequency of the main valve, which is 1671Hz calculated by Eq. (14), is far quicker than that of the pilot valve, the pressure of the control chamber soon reaches a steady state during the response time of the pilot valve. So the dynamic characteristics of the main stage can be simplified as a first order system [23]. All flow rate of the pilot stage in addition to leakage is used to drive the main valve spool, so the kinematics equation of the main valve spool can be written as Eq. (15).

$$f_p = \frac{1}{2\pi}\sqrt{\frac{4\beta_e A_V^{\ 2}}{V_0 M}} \tag{14}$$

$$\dot{x}_{\mathrm{m}} = \frac{q_{\mathrm{p}}}{A_{\mathrm{m}}} - \frac{q_{\mathrm{leak}}}{A_{\mathrm{m}}} + d_{\mathrm{m}} \tag{15}$$

In Eq.(15) $q_{\mathrm{p}}$ is the flow rate of the pilot stage, $q_{\mathrm{leak}}$ is the leakage, $d_{\mathrm{m}}$ is the disturbance of the system. Eq. (15) is convenient for designing the main valve spool position control strategy based on the flow rate characteristic of the pilot valve.

According to the first order state equation (15), the main task of the position control of the main valve spool is to design an appropriate control law of $q_{\mathrm{p}}$. This control law calculates the desired pilot valve flow rate $q_{\mathrm{pd}}$ that satisfies the requirement of the main valve position control, which can be called as desired flow rate generator. Then the following task is to design a pilot valve flow rate controller, whose outputs are the desired currents $I_{\mathrm{Ad}}$, $I_{\mathrm{Bd}}$ of the two solenoids, to track the desired flow rate $q_{\mathrm{pd}}$. Finally, the rest task is to use the PI current controller to track the desired currents of the solenoids [24]. Then the force of the solenoid drives the pilot valve spool to achieve the corresponding desired displacement and obtain the corresponding flow rate, so as to realize the closed-loop position control of the main valve spool. This framework of the closed-loop position control of the main valve spool is shown in Fig. 10.

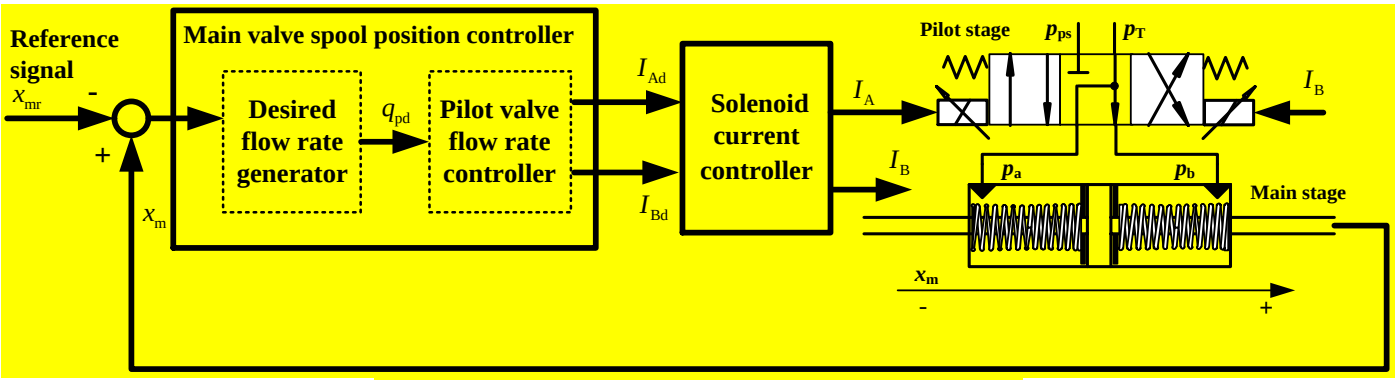


**Fig. 10. The framework of the main valve spool position control**

The framework includes the outer loop controller of the main valve spool position and the inner loop controller of the solenoid current. The outer loop controller, which outputs the desired input current of the inner loop controller, consists of two parts: the desired flow rate generator and the pilot valve flow rate controller. In this paper, the pilot valve flow rate controller calculates the desired current $I_{\mathrm{Ad}}$, $I_{\mathrm{Bd}}$ of the pilot valve by an open-loop projection method based on the calibrated flow rate characteristic of the pilot valve, as Eq. (16) shows.

$$\left[I_{\mathrm{Ad}}, I_{\mathrm{Bd}}\right] = f_{\mathrm{id}}^{-1}(\mathrm{Sat}(\frac{q_{\mathrm{pd}}}{A_{\mathrm{m}}})) = \begin{cases} \left[I_{\mathrm{Ad}} = f^{-1}{}_{\mathrm{A1}}(\mathrm{Sat}_{\mathrm{A1}}(\frac{q_{\mathrm{pd}}}{A_{\mathrm{m}}})), I_{\mathrm{Bd}} = 0\right], \text{if } x_{\mathrm{m}} > 0, \quad q_{\mathrm{pd}} > 0 \\ \left[I_{\mathrm{Ad}} = f^{-1}{}_{\mathrm{A2}}(\mathrm{Sat}_{\mathrm{A2}}(\frac{q_{\mathrm{pd}}}{A_{\mathrm{m}}})), I_{\mathrm{Bd}} = 0\right], \text{if } x_{\mathrm{m}} > 0, \quad q_{\mathrm{pd}} < 0 \\ \left[I_{\mathrm{Ad}} = 0, I_{\mathrm{Bd}} = 0\right], \text{if } x_{\mathrm{m}} = 0 \\ \left[I_{\mathrm{Ad}} = 0, I_{\mathrm{Bd}} = f^{-1}{}_{\mathrm{B2}}(\mathrm{Sat}_{\mathrm{B2}}(\frac{q_{\mathrm{pd}}}{A_{\mathrm{m}}}))\right], \text{if } x_{\mathrm{m}} < 0, \quad q_{\mathrm{pd}} > 0 \\ \left[I_{\mathrm{Ad}} = 0, I_{\mathrm{Bd}} = f^{-1}{}_{\mathrm{B1}}(\mathrm{Sat}_{\mathrm{B1}}(\frac{q_{\mathrm{pd}}}{A_{\mathrm{m}}}))\right], \text{if } x_{\mathrm{m}} < 0, \quad q_{\mathrm{pd}} < 0 \end{cases} \tag{16}$$

where $f_{\mathrm{id}}(I_{\mathrm{A}}, I_{\mathrm{B}})$ is the calibrated flow rate characteristic of the pilot stage as shown in Fig. 9 in section 3; $\mathrm{Sat}_{\mathrm{A1}}(\bullet)$, $\mathrm{Sat}_{\mathrm{A2}}(\bullet)$, $\mathrm{Sat}_{\mathrm{B1}}(\bullet)$, $\mathrm{Sat}_{\mathrm{B2}}(\bullet)$ are the corresponding nonlinear saturation functions considering the bounded calibrated flow rate, they have the form

$$v_{\mathrm{m}} = \mathrm{Sat}_{\mathrm{xx}}(\frac{q_{\mathrm{pd}}}{A_{\mathrm{m}}}) = \begin{cases} v_{\mathrm{maxxx}}, & \text{if } \frac{q_{\mathrm{pd}}}{A_{\mathrm{m}}} > v_{\mathrm{maxx}} \\ \frac{q_{\mathrm{pd}}}{A_{\mathrm{m}}}, & \text{if } v_{\mathrm{minxx}} \le \frac{q_{\mathrm{pd}}}{A_{\mathrm{m}}} \le v_{\mathrm{maxxx}} \\ v_{\mathrm{minxx}}, & \text{if } \frac{q_{\mathrm{pd}}}{A_{\mathrm{m}}} < v_{\mathrm{minxx}} \end{cases}. \tag{17}$$

In Eq. (17), the subscript xx represents A1, A2, B1, B2; $v_{\mathrm{maxxx}}$, $v_{\mathrm{minxx}}$ are the maximum and minimum calibrated flow rate of the corresponding detection process. In practice, the flow rate characteristics are applied in the valve digital controller by the interpolation method of look-up table. By using this control method, the micro flow rate (MFR) of the intermediate deadzone has been concerned, which eliminates the discontinuity and unsmooth domain in the previous inverse deadzone compensation function and avoids the selection of the threshold value during the deadzone detection.

The desired flow rate generator can be designed as described below. When the main valve spool tracks the reference position $x_{\mathrm{mr}}$, defining error $e_1 = x_{\mathrm{m}} - x_{\mathrm{mr}}$, $e_2 = \dot{e}_1$ and introducing the error integrals $\sigma$, Eq. (15) is extended to

$$\begin{bmatrix} \dot{\sigma} \\ \dot{e}_1 \end{bmatrix} = \begin{bmatrix} 0 & 1 \\ 0 & 0 \end{bmatrix} \begin{bmatrix} \sigma \\ e_1 \end{bmatrix} + \begin{bmatrix} 0 \\ \frac{f_{\mathrm{id}}(I_{\mathrm{A}}, I_{\mathrm{B}}) + d_{\mathrm{q}}}{A_{\mathrm{m}}} - \frac{q_{\mathrm{leak}}}{A_{\mathrm{m}}} + d_{\mathrm{m}} - \dot{x}_{\mathrm{mr}} \end{bmatrix}, \tag{18}$$

where $d_{\mathrm{q}}$ is disturbance and error between the calibrated pilot flow rate and the real pilot flow rate. The sum of $f_{id}$ and $d_{\mathrm{q}}$ is used to characterize the flow rate $q_{\mathrm{p}}$.

To design the control law of $I$, the slide mode is designed as

$$S = K_{\mathrm{I}}\sigma + K_{\mathrm{P}}e_1 + e_2 = 0, \tag{19}$$

where $K_{\mathrm{I}}$, $K_{\mathrm{P}}$ are greater than zero and guarantee that $\begin{bmatrix} 0 & 1 \\ -K_{\mathrm{I}} & -K_{\mathrm{P}} \end{bmatrix}$ is Hurwitz. Then define the Lyapunov function of the slide mode as $V = \frac{1}{2}S^2$, and its derivative is

$$\dot{V} = S\dot{S} = S\left(K_{\mathrm{I}}e_1 + K_{\mathrm{P}}e_2 + \dot{e}_2\right) = SK_{\mathrm{P}}\frac{f_{\mathrm{id}}(I_{\mathrm{A}}, I_{\mathrm{B}})}{A_{\mathrm{m}}} + S\left(K_{\mathrm{P}}\left(\frac{d_{\mathrm{q}}}{A_{\mathrm{m}}} - \frac{q_{\mathrm{leak}}}{A_{\mathrm{m}}} + d_{\mathrm{m}} - \dot{x}_{\mathrm{mr}}\right) + \dot{e}_2 + K_{\mathrm{I}}e_1\right). \tag{20}$$

If

$$\left| \frac{K_{\mathrm{P}}\left(\frac{d_{\mathrm{q}}}{A_{\mathrm{m}}}-\frac{q_{\mathrm{leak}}}{A_{\mathrm{m}}}+d_{\mathrm{m}}-\dot{x}_{\mathrm{mr}}\right)+\dot{e}_2+K_{\mathrm{I}}e_1}{\frac{K_{\mathrm{P}}}{A_{\mathrm{m}}}} \right| < K_0 \quad , \tag{21}$$

then

$$\dot{V}=SK_{\mathrm{P}}\frac{f_{\mathrm{id}}(I_{\mathrm{A}},I_{\mathrm{B}})}{A_{\mathrm{m}}}+S\left(K_{\mathrm{P}}\left(\frac{d_{\mathrm{q}}}{A_{\mathrm{m}}}-\frac{q_{\mathrm{leak}}}{A_{\mathrm{m}}}+d_{\mathrm{m}}-\dot{x}_{\mathrm{mr}}\right)+\dot{e}_2+K_{\mathrm{I}}e_1\right)<S\left(K_{\mathrm{P}}\frac{f_{\mathrm{id}}(I_{\mathrm{A}},I_{\mathrm{B}})}{A_{\mathrm{m}}}\right)+K_0\frac{K_{\mathrm{P}}}{A_{\mathrm{m}}}S\,\mathrm{sign}(S) \quad . \tag{22}$$

Thus the desired flow rate $q_{\mathrm{pd}}$ can be designed as

$$q_{\mathrm{pd}}=f_{\mathrm{id}}(I_{\mathrm{A}},I_{\mathrm{B}})A_{\mathrm{m}}=-K_0A_{\mathrm{m}}\,\mathrm{sign}(S) \quad , \tag{23}$$

which can guarantee that derivative of the Lypunove function is smaller than zero. To eliminate chattering of control performance, the signum function can be approximated by the high-slope saturation function [25], and the desired flow rate $q_{\mathrm{pd}}$ can be rewritten as

$$q_{\mathrm{pd}}=f_{\mathrm{id}}(I_{\mathrm{A}},I_{\mathrm{B}})A_{\mathrm{m}}=-K_0A_{\mathrm{m}}\mathrm{sat}\left(\frac{S}{\xi}\right) \quad , \tag{24}$$

where $\xi$ is a small positive value. Substituting (19) in to (24), the control law of the desired flow rate $q_{\mathrm{pd}}$ is a PID controller followed by saturation with gain $K_0$, as shown below.

$$q_{\mathrm{pd}}=f_{\mathrm{id}}(I_{\mathrm{A}},I_{\mathrm{B}})A_{\mathrm{m}}=-K_0A_{\mathrm{m}}\mathrm{sat}\left(\frac{K_{\mathrm{I}}}{\xi}\sigma+\frac{K_{\mathrm{P}}}{\xi}e_1+\frac{1}{\xi}e_2\right) \tag{25}$$

The schematic of the closed-loop position control of the main valve spool, which contains the deadzone compensation control strategy with calibrated flow rate characteristic of the pilot valve, is shown in Fig. 11. According to the difference between the reference main valve spool displacement $x_{\mathrm{mr}}$ and the actual displacement $x_{\mathrm{m}}$, the desired flow rate generator calculates the required flow rate $q_{\mathrm{pd}}$ to drive the main valve spool by Eq. (25). Then according to $q_{\mathrm{pd}}$, the pilot valve flow rate controller calculates the desired current $I_{\mathrm{Ad}}$, $I_{\mathrm{Bd}}$ of the solenoids by Eq. (16), which is an open-loop projection method based on the calibrated flow rate characteristic as shown in Fig.9. Since the calibrated flow rate characteristic contains the information of micro flow rate at the intermediate position, the deadzone compensation considering the micro flow rate is realized. Finally, the inner loop solenoid current controller tracks the desired current $I_{\mathrm{Ad}}$, $I_{\mathrm{Bd}}$ and the closed-loop position control of the main valve spool is realized.

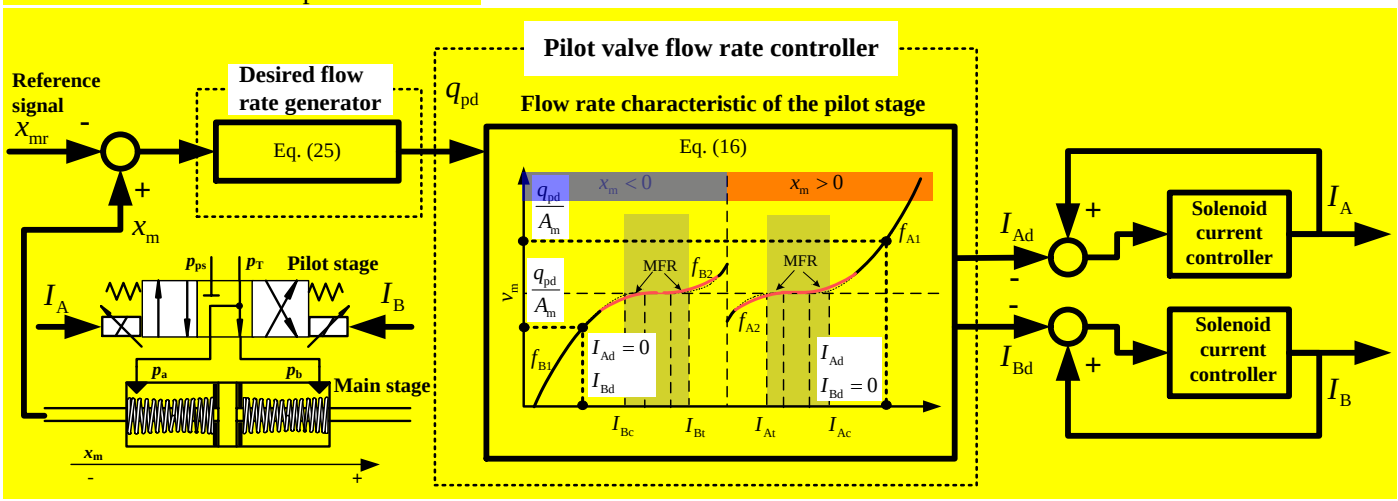


**Fig. 11. The schematic of the main valve spool position control.**

# 5 Experimental verification

## 5.1 Experimental set-up and parameter settings

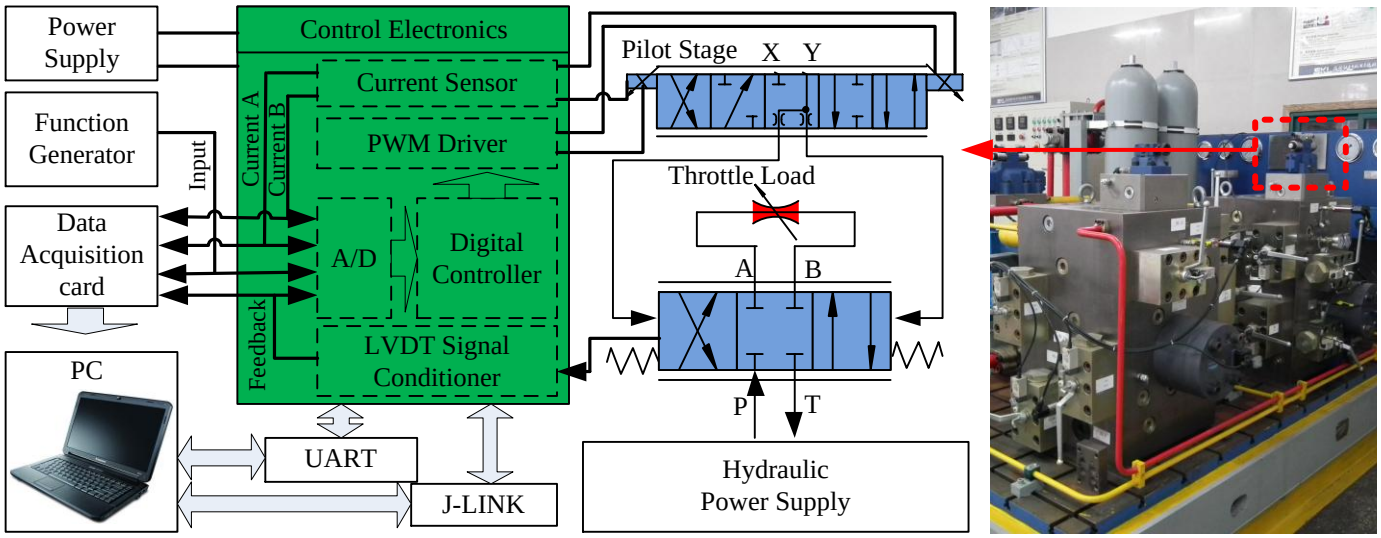


**Fig. 12. The schematic diagram of the experimental setup and test rig.**

The schematic diagram of the system and the experimental setup used in the experiments are the same as the previous research as shown in Fig. 12. The function generator is used to produce an analogue signal as the reference signal to the digital controller. The microcontroller is an ARM-based 32-bit MCU with 128KB Flash. All the control functions including current controller and position controller are embedded in this MCU. The PWM modulator is also integrated in the control electronics. The solenoid is driven by the PWM modulator to generate a PWM signal with controlled duty cycle. The LVDT signal conditioner is used to convert the main valve spool displacement to an analogy signal.

A 16-bit data acquisition card (DAC) with USB interface is used to sample the required signals including: the input reference signal, the main spool position and the solenoid currents in the left and right solenoids. Besides, the UART (Universal Asynchronous Receiver/Transmitter) is used for communication between PC and the digital controller. Both of the current sensors for two solenoids have been calibrated with a high-precision ampere meter. The LVDT signal conditioner has also been adjusted from ±5mm to ±10V.

In order to give general comparative results, the hydraulic power supply and the oil temperature are set in a typical condition. The maximum pressure is set as 10MPa and the flow rate is controlled at 200L/min as initial condition.

The parameters $K_0$, $K_I$, $K_P$, $\xi$ in the control law Eq. (25) are determined as follows. $K_P$, $K_I$ are set as 100 and 10 respectively to guarantee the convergences of the error $e$ in 50ms under the dynamic of the slide mode surface. $K_0$ is set as 6.87 in the case that the flow rate unit is L/min. The value of $K_0$ is estimated by the detection results of pilot valve flow rate characteristic, which is not bigger than 200mm/s. $\xi$ is increased from a small value until eliminating the chattering of control performance, and it is set as 0.1 finally.

## 5.2 Experimental results

Comparison of the two deadzone compensation methods are as follows: the first one uses Eq. (9) in the control law, which is without the micro flow rate at the intermediate position (without MFR); the other one uses Eq. (16) in the control law, which is with the micro flow rate at the intermediate position (with MFR). In the experiment, the desired flow rate generator adopts a PID controller as Eq. (25), and the solenoid current also adopts a PI controller [24]. The PID and PI controllers of both methods use the same parameters. The solenoid current PI controller which is adjusted by the Ziegler Nichols [26, 27] tuning procedure initially and manually optimized later. The proportional gain and the integral gain are 32.02, 1.02 in the case that the current unit is mA and 100% PWM duty ratio is equivalent to 10000.

Figs. 13-15 are the steady-state tracking results of the main valve spool displacement. The sampling frequency of the signal is 1 kHz. The red curve is the results of control method with MFR, and the blue curve is the results of control method

without MFR. During the processes of the deadzone detection, the threshold values of the main valve spool displacement are set as 0.5%, 2% and 3% respectively, in the case that $X_m$ is at 90% stroke. The experimental results in Table 3 and Figs. 13-15 are obtained. According to Table 3, the detected deadzone values $I_{Ac}$, $I_{Bc}$ increase with the increment of the threshold, and the detected deadzone values $I_{At}$, $I_{Bt}$ decrease with the increment of the threshold. It is because that the threshold value leads the additional flow rate into the process of deadzone detection. The detected deadzone values affected by the threshold value also verify the theoretical deduction in the second section of this paper. The deadzones of the pilot valve port A, B are asymmetric, that the deazone of port A is wider than that of port B, as shown in Table 3. The asymmetry is due to the manufacturing variation of the valve and characteristic difference of solenoids.

The steady-state position tracking performances of the main valve spool under different threshold values are shown in Figs. 13-15. In these figures, (a) and (b) show the main valve spool displacement at the positive position and negative position respectively, (c) and (d) indicate the current of the corresponding solenoid. The steady-state tracking accuracy of the control method with MFR is better than that without MFR. As the threshold value increased, the tracking accuracy of the control method without MFR is worsened. But the steady-state tracking accuracy of the control method with MFR is almost unchanged under different threshold values. The solenoid currents of the control method with MFR have smaller amplitude and less intense vibration than that without MFR. And as the detected deadzones widen as threshold values increase, the solenoid currents of the control method without MFR have larger amplitude and more intense vibration, which is due to the vibration of the detected deadzone values in Eq. (9). These current responses reveal that the control method with MFR eliminates discontinuity and unsmooth domain in inverse deadzone compensation, thus improves the current control performance, so the performance of the main valve spool position control is improved. Additionally, the solenoid currents of the control method with MFR have less intense vibration as threshold values increase. It is due to the increment of the overlapped region between the driving flow characteristic and the damping flow characteristic. The two flow characteristics are calibrated with the solenoid current starting from the detected deadzone values $I_{A(B)c}$ in the improved deadzone detection method. So the overlapped region of the flow characteristics increases as $I_{A(B)c}$ decreases as shown in Table 3. And the more overlapped region of the flow characteristics makes current calculated by Eq. (16) change more smoothly when conditions of Eq. (16) change. What's more, the tracking performances at the positive position and negative position also reflect the asymmetry of the valve. Table 3 gives a statistical analysis of the steady-state tracking error. It is shown that the steady-state tracking accuracy is greatly improved by the control method with MFR.

The sinusoidal position tracking of the main valve spool is shown in Fig. 16, where (a) is the main valve spool displacement and (b) is the currents of the corresponding solenoid. The threshold values of the main valve spool displacement are set as 0.5%. According to Fig. 16(b), the solenoid currents of the control method with MFR have less intense vibration than that without MFR, especially in the first quarter of a sinusoidal cycle. It is because that the desired solenoid current calculated by Eq. (9) in the control method without MFR has an unsmooth domain in the neighborhood of $q_{pd}$=0. The more intense current vibration of the control method without MFR in the first quarter of a sinusoidal cycle is due to the large length of ($I_{Ac}$-$I_{At}$), as shown in Table 3. The position tracking curve of the control method with MFR is smoother than that without MFR, especially when the main valve spool crosses the zero position. And the phase delay with MFR is less than that without MFR in the second and fourth quarter of a sinusoidal cycle. During these quarters, the main valve spool position is driven by the damping flow of the pilot valve, and the control method with MFR is more sensitive to small position error of the main valve spool. The solenoid current vibrations in the second and fourth quarter of a sinusoidal cycle show the control effect, so the control method with MFR gets a better tracking performance.

**Table 3 Detected deadzone values and square root of tracking error**

| Threshold(%) | $I_{Ac}$; $I_{At}$(mA) | $I_{Bc}$; $I_{Bt}$(mA) | $x_{mr}$ (%) | SRE(%) without MFR | SRE(%) with MFR |
|---|---|---|---|---|---|
| 0.5 | 1713;1422 | 1540;1393 | 50 | 0.201 | 0.083 |
| | | | -50 | 0.139 | 0.115 |
| 2 | 1745;1361 | 1569;1339 | 50 | 0.182 | 0.077 |
| | | | -50 | 0.172 | 0.11 |
| 3 | 1768;1332 | 1588;1287 | 50 | 0.372 | 0.08 |
| | | | -50 | 0.202 | 0.125 |

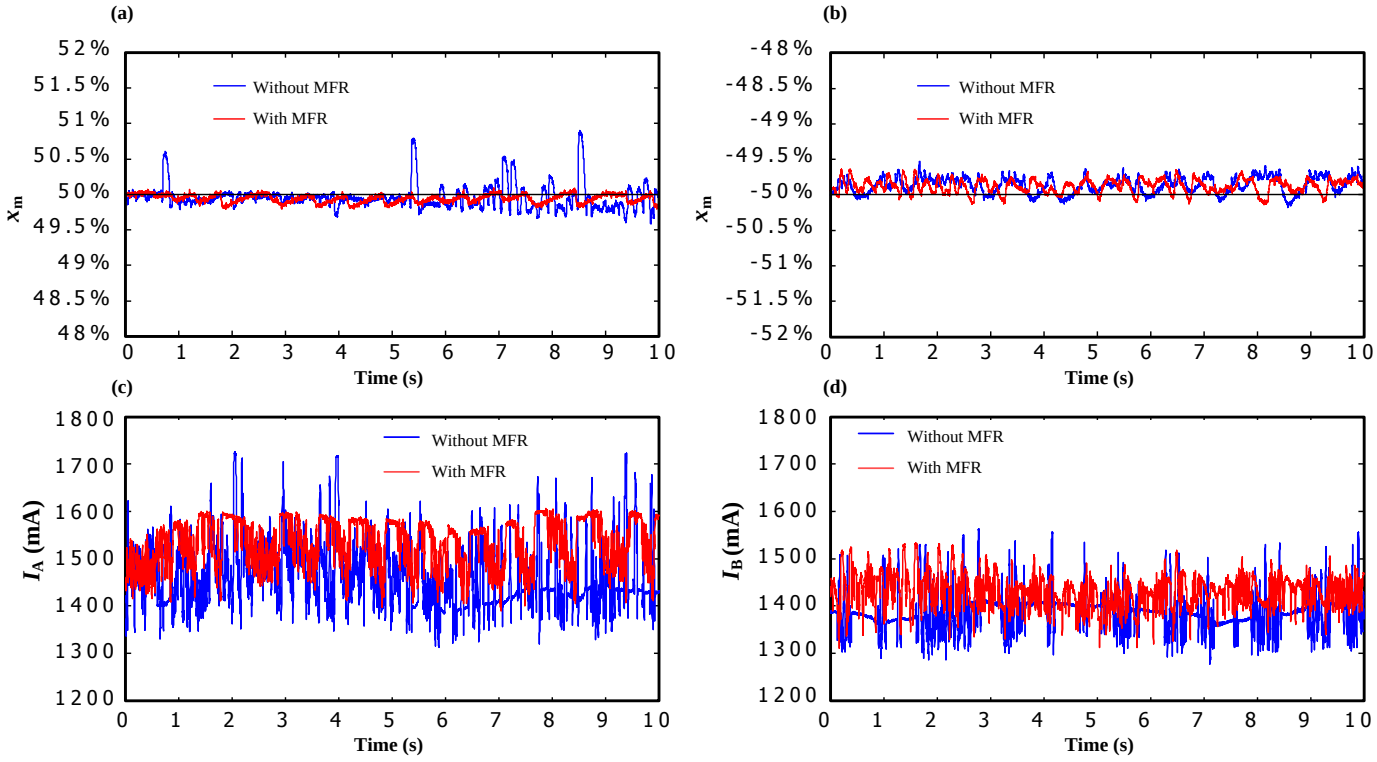


**Fig. 13. Experimental results of steady-state tracking with 0.5% threshold value.**

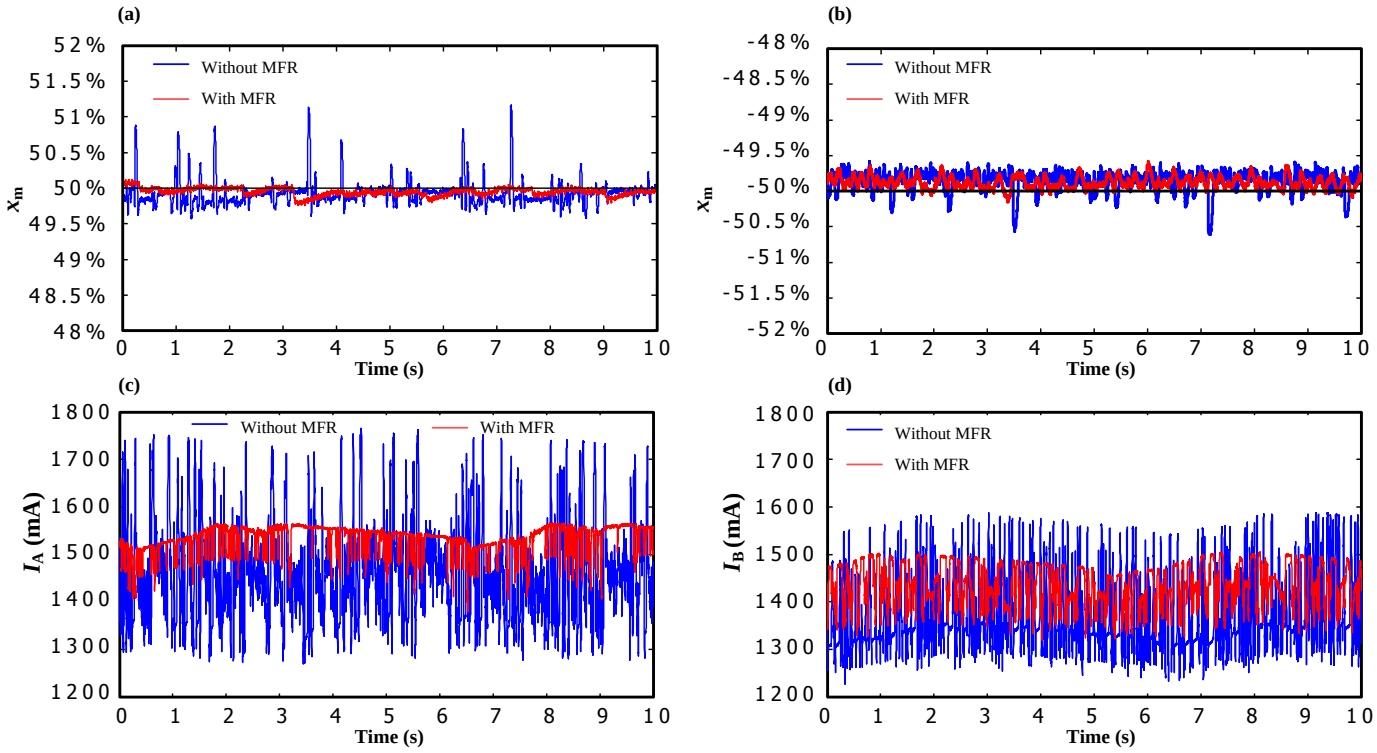


**Fig. 14. Experimental results of steady-state tracking with 2% threshold value.**

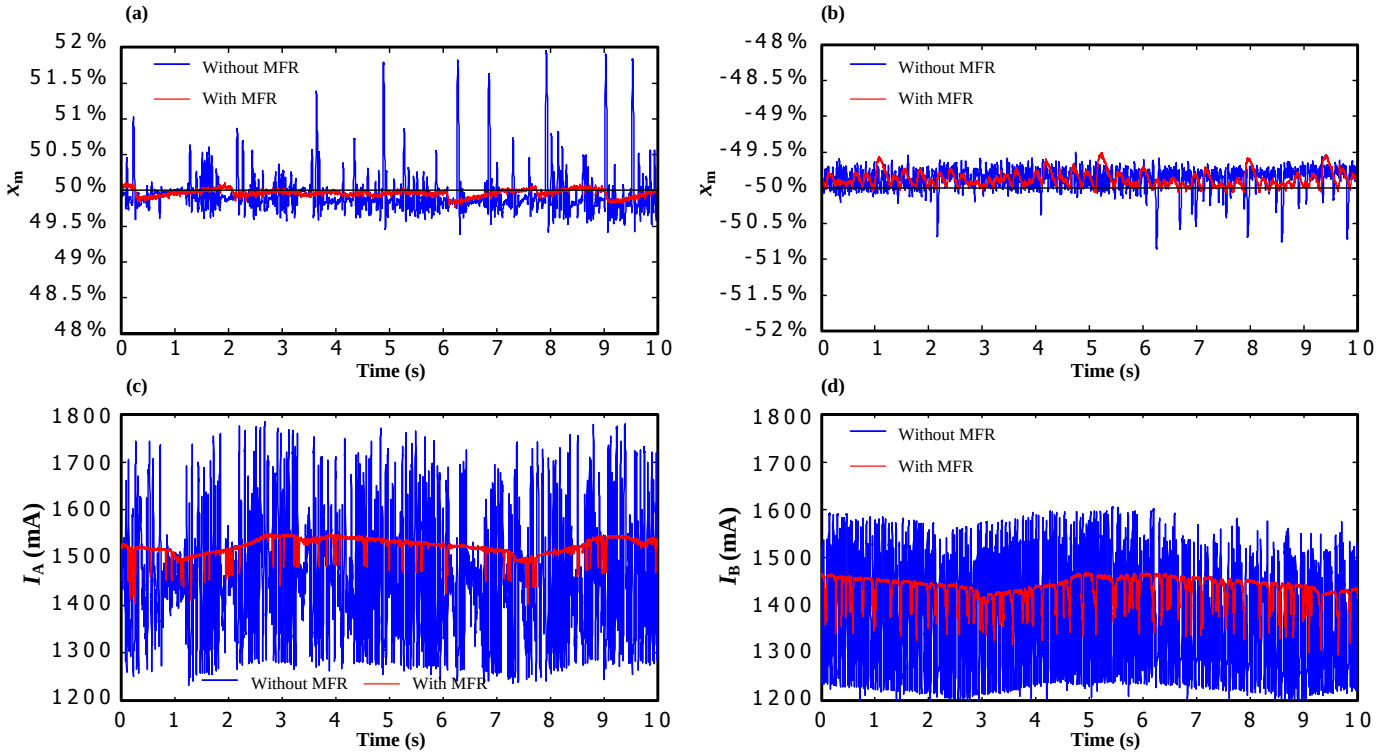


**Fig. 15. Experimental results of steady-state tracking with 3% threshold value**

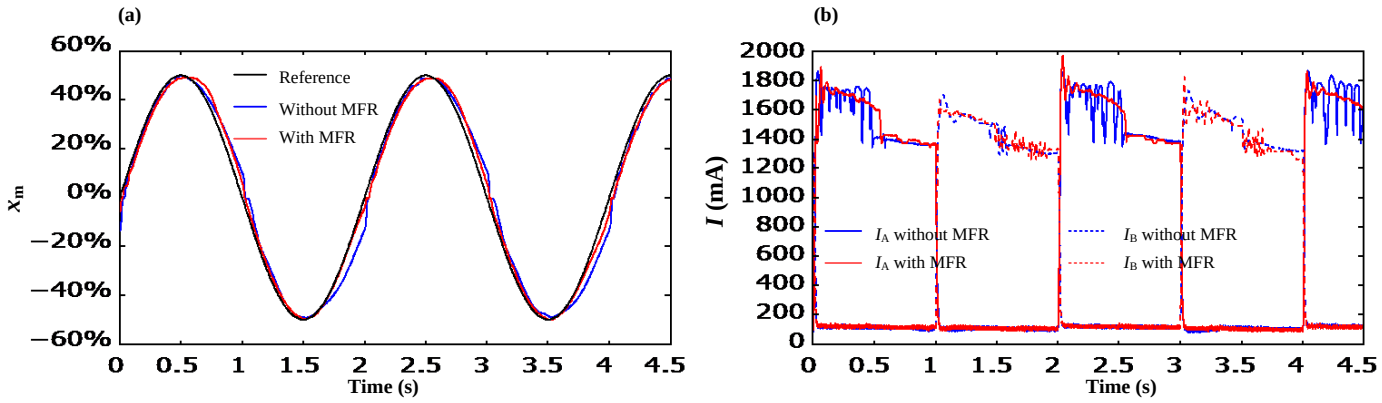


**Fig. 16. Experimental results of sinusoidal tracking.**

# 6 Conclusion

In the previous research, we propose a deadzone compensation method for the pilot stage of the proportional valve based on a cascade deadzone model. This method effectively narrows the tracking error of the main valve spool position and the tracking lag at the direction changing moment of main valve spool motion. However, two aspects for the cascade deadzone model can be modified to further improve the control accuracy of the main valve. Firstly, due to the gap and leakage of the pilot valve, there is micro flow rate due to the difference between the actual deadzone values and overlaps at the intermediate position. The micro flow rate is simplified as zero by the compensation method. This simplification introduces discontinuity and unsmooth domain in the control of the solenoid current, and affects the accuracy of the position control of the main valve spool. Secondly, the threshold selection of the main valve spool displacement in the detection process of the deadzones affects the detected deadzone values, thus it affects the position control accuracy of the main valve spool. This paper aims to further improve the control accuracy of the main valve, and the following conclusions are drawn.

(1) Because of the gap and the leakage of the pilot valve, the micro flow rate exists at the intermediate position of the pilot valve. The micro flow rate is helpful to eliminate the discontinuity and unsmooth domain in the previous inverse deadzone compensation function.

(2) In order to calibrate the flow characteristics of the pilot valve which include the micro flow rate, an improved deadzone detection method is proposed. Its detection processes are realized according to two principles. First, the pilot flow rate is characterized by the main valve spool speed; second, the pilot valve displacement is characterized by the solenoid current. This deadzone detection method avoids selection of an appropriate threshold value of the main valve spool displacement. And the calibrated flow characteristics of the pilot valve contain the information of the micro flow rate and the deadzone, so the calibration results are useful for the control strategy of deadzone compensation.

(3) The deadzone compensation control strategy with calibrated flow rate characteristic of the pilot valve is proposed. The outer loop of this framework consists of the pilot valve flow rate controller and the desired flow rate generator. The pilot valve flow rate controller is designed based on the calibrated flow characteristics of the pilot valve, so it can compensate the deadzone. The desired flow rate generator is developed using sliding mode method, and it is a PID controller followed by saturation.

(4) The experimental results including both steady-state position tracking and sinusoidal position tracking show that the proposed control strategy with MFR, which eliminates the discontinuity and unsmooth domain in the inverse deadzone function, effectively improves the tracking accuracy of the position control of the main valve spool.

# Acknowledgements

The authors gratefully acknowledge the support of the NSFC-Zhejiang Joint Fund for the Integration of

Industrialization and Informatization [No. U1509204], the National Natural Science Foundation of China [No.91748210, No.51805470].

# References

[1] N. Manring. Hydraulic control systems. John Wiley & Sons, New York; 2005.
[2] V.R.P.E. Dominick, V.R.P.H.D. Donald, G.R.P.E. Marlene. Injection Molding Handbook, Springer US; 2000.p. 35-85.
[3] Zavarehi M K, Lawrence P D, Sassani F. Nonlinear modeling and validation of solenoid-controlled pilot-operated servovalves. IEEE-ASME Trans. Mechatron 1999;4(3):324-334.
[4] J.B. Gamble. Comparison of Sliding Mode Control With State Feedback and PID Control Applied to a Proportional Solenoid Valve. J. Dyn. Syst. Meas. Control-Trans. ASME 1996; 118(3):434-438.
[5] J.H. Fang, Z. Chen and J.H. Wei. Some practical improvements of sliding-mode control for servo-solenoid valve. Proc. Inst. Mech. Eng. Part I-J Syst Control Eng 2016;230(7).
[6] C. Krimpmann, G. Schoppel, I. Glowatzky and T. Bertram. Performance evaluation of nonlinear surfaces for sliding mode control of a hydraulic valve. In: Control Applications (CCA), IEEE Conference on; 2015.
[7] C. Krimpmann, G. Schoppel, I. Glowatzky and T. Bertram, Lyapunov-based self-tuning of sliding surfaces—methodology and application to hydraulic valves. In: Advanced Intelligent Mechatronics (AIM), IEEE International Conference on; 2016 .
[8] I. Lee, D. Oh, S. Ji and S. Yun. Control of an overlap-type proportional directional control valve using input shaping filter. Mechatronics 2015;29:87-95.
[9] Genmao W, Xiumin Q, Qingfeng W, Jianhua W, Xiaowu K, Xin F. Electrohydraulic proportional technique in theory and application. Zhejiang University Press;2006.
[10] J.D. Fortgang, L.E. George and W.J. Book. Practical implementation of a dead zone inverse on a hydraulic wrist. In: ASME International Mechanical Engineering Congress and Exposition; 2002 .
[11] G.P. Liu and S. Daley. Optimal-tuning nonlinear PID control of hydraulic systems. Control Eng. Practice 2000;8(9):1045-1053.
[12] B. Xu, Q. Su, J. Zhang and Z. Lu. A dead-band model and its online detection for the pilot stage of a two-stage directional flow control valve. Proc. Inst. Mech. Eng. Part C-J. Eng. Mech. Eng. Sci 2016;230(4):1989-1996.
[13] J.D.J. Rubio, Z. Zamudio, J. Pacheco and D. Mújica Vargas. Proportional Derivative Control with Inverse Dead-Zone for Pendulum Systems. Math Probl Eng 2013;(5):1-9.
[14] X. Zhao, P. Shi, X. Zheng and L. Zhang. Adaptive tracking control for switched stochastic nonlinear systems with unknown actuator dead-zone. Automatica 2015;60(C):193-200.
[15] H. Yan and Y. Li. Adaptive NN prescribed performance control for nonlinear systems with output dead zone. Neural Comput Appl 2017;28:145-153.
[16] J. Na, X. Ren, G. Herrmann and Z. Qiao. Adaptive neural dynamic surface control for servo systems with unknown dead-zone, Control Eng Pract 2011;19:1328-1343.
[17] J.H. Pérez-Cruz, E. Ruiz-Velázquez, J.D.J. Rubio and C.A. de Alba-Padilla. Robust Adaptive Neurocontrol of SISO Nonlinear Systems Preceded by Unknown Deadzone. Math Probl Eng 2012; 7:1-23.
[18] Q. Chen, X. Ren, J. Na and D. Zheng. Adaptive robust finite-time neural control of uncertain PMSM servo system with nonlinear dead zone. Neural Comput Appl 2016; 1-12.
[19] Cruz J H P, Avila J D J R, Flores J L, et al. Control of Uncertain Plants with Unknown Deadzone via Differential Neural Networks. IEEE Latin Am. Trans 2015; 13(7):2085-2093.
[20] Peng J, Dubay R. Identification and adaptive neural network control of a DC motor system with dead-zone characteristics. ISA Trans 2011;50(4):588-598.
[21] B. Xu, Q. Su, J. Zhang and Z. Lu. Analysis and compensation for the cascade dead-zones in the proportional control valve. ISA Trans 2017;66:393.
[22] Tao G, Kokotović P V. Adaptive Control of Plants with Unknown Dead-zones. In: American Control Conference, IEEE;

1992:2710-2714.
[23] Fang, Jing Hui. The Design and Control Strategy Study of the Large-flow Cartridge Servo Valve. Zhejiang University; 2013.Ph.D. thesis.
[24] J. Zhang, Z. Lu, B. Xu, Q. Su, D. Wang, P. Min. Investigation Into the Nonlinear Characteristics of a High-Speed Drive Circuit for a Proportional Solenoid Controlled by a PWM Signal. IEEE Access 2018;6: 61665-61676.
[25] H.K. Khalil and J.W. Grizzle, Nonlinear systems, vol. 3, Prentice hall New Jersey, 1996 .
[26] Åström K J, Hägglund T. Automatic tuning of simple regulators with specifications on phase and amplitude margins. Automatica 1984; 20(5):645-651.
[27] Ziegler J G. Optimum Settings for Automatic Controllers. Asme Trans 1942; 64(2B):759-768 .

# Figure captions

**Figure 1**

Click here to download high resolution image

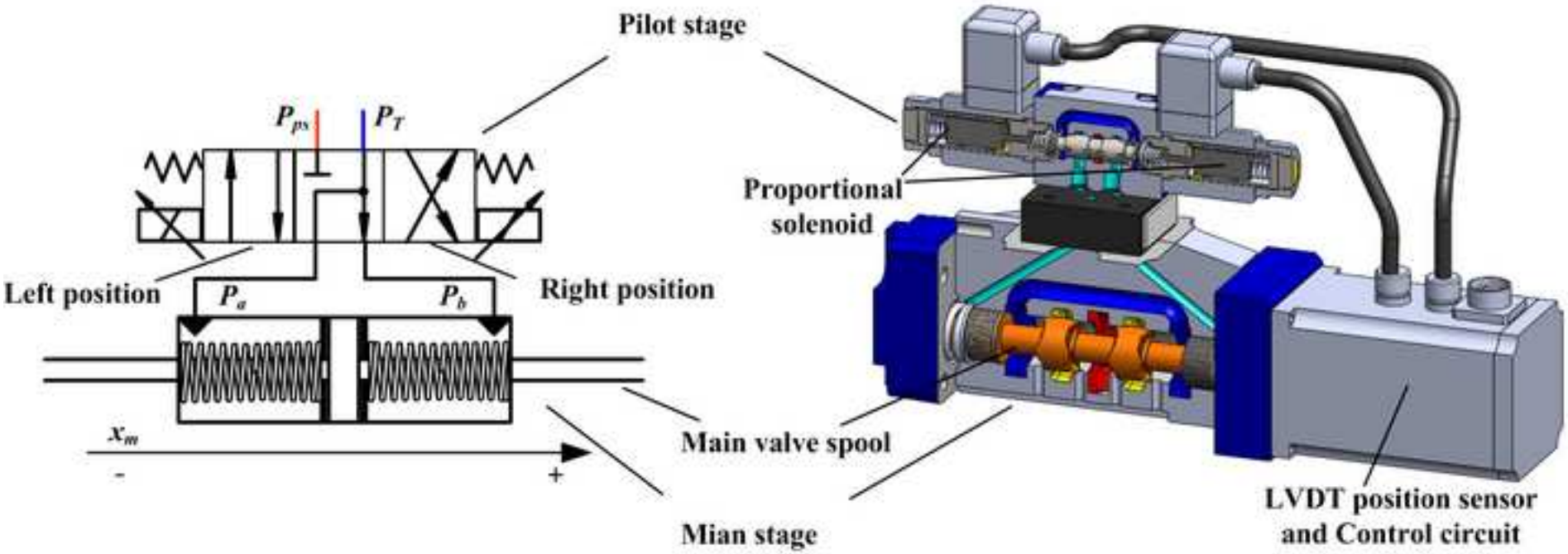

Figure 2

Click here to download high resolution image

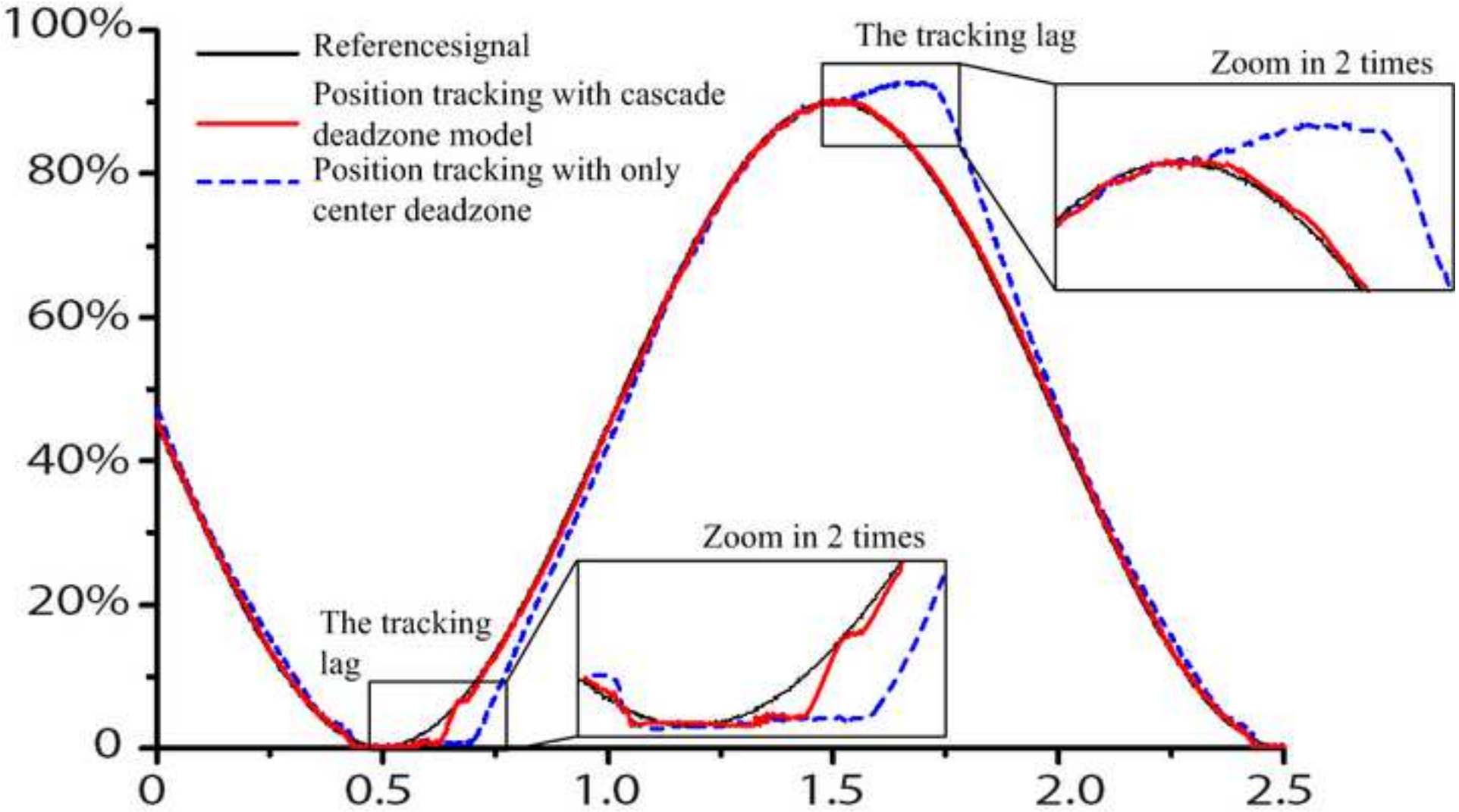

Figure 3

Click here to download high resolution image

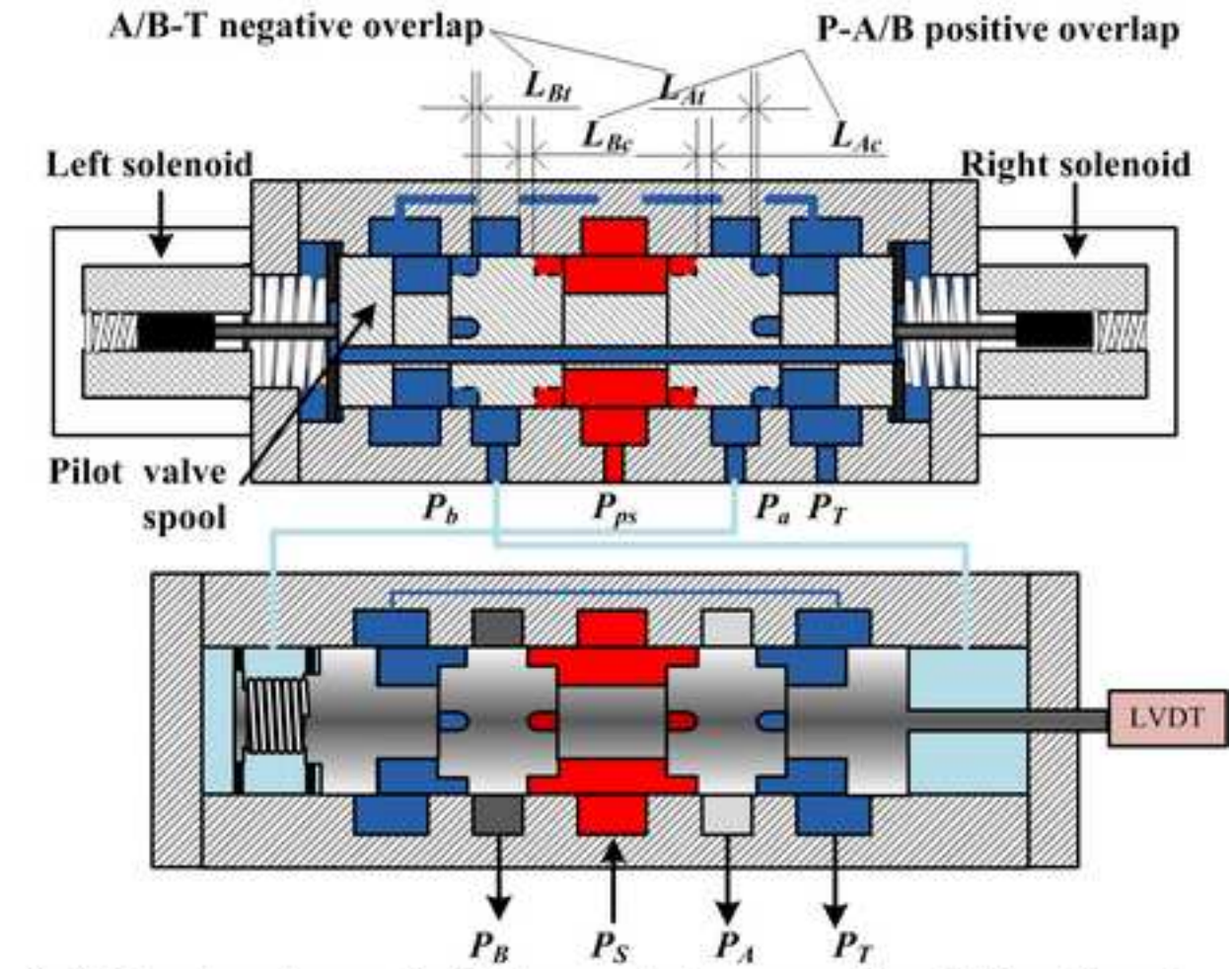


(a) The structure of pilot operated proportional directional valve with overlaps

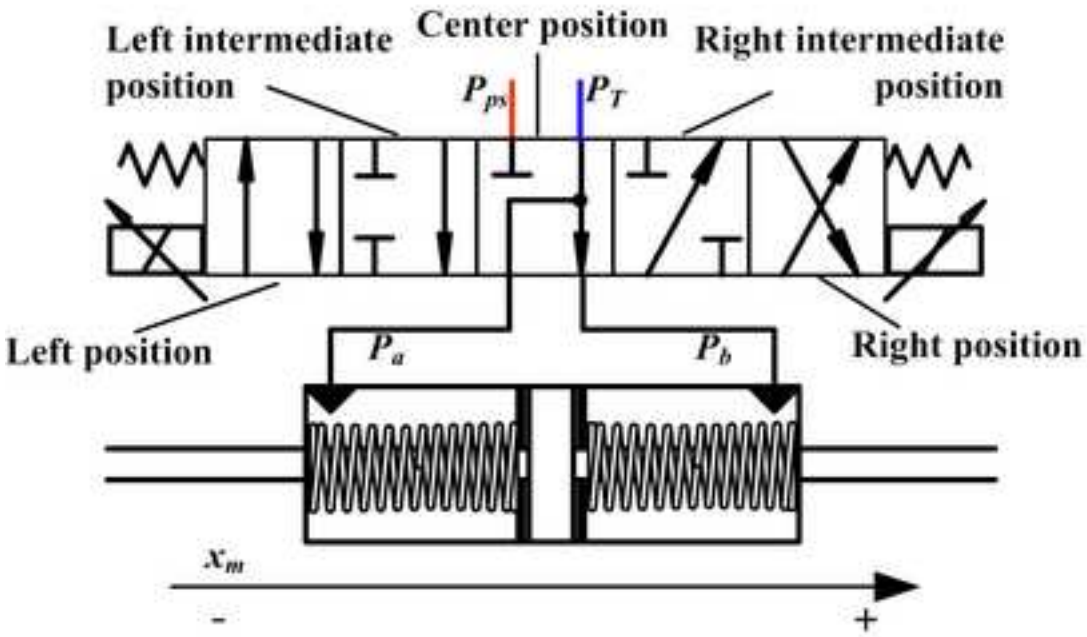


(b) The schematic of the valve with detailed pilot valve working positons

Figure 4

Click here to download high resolution image

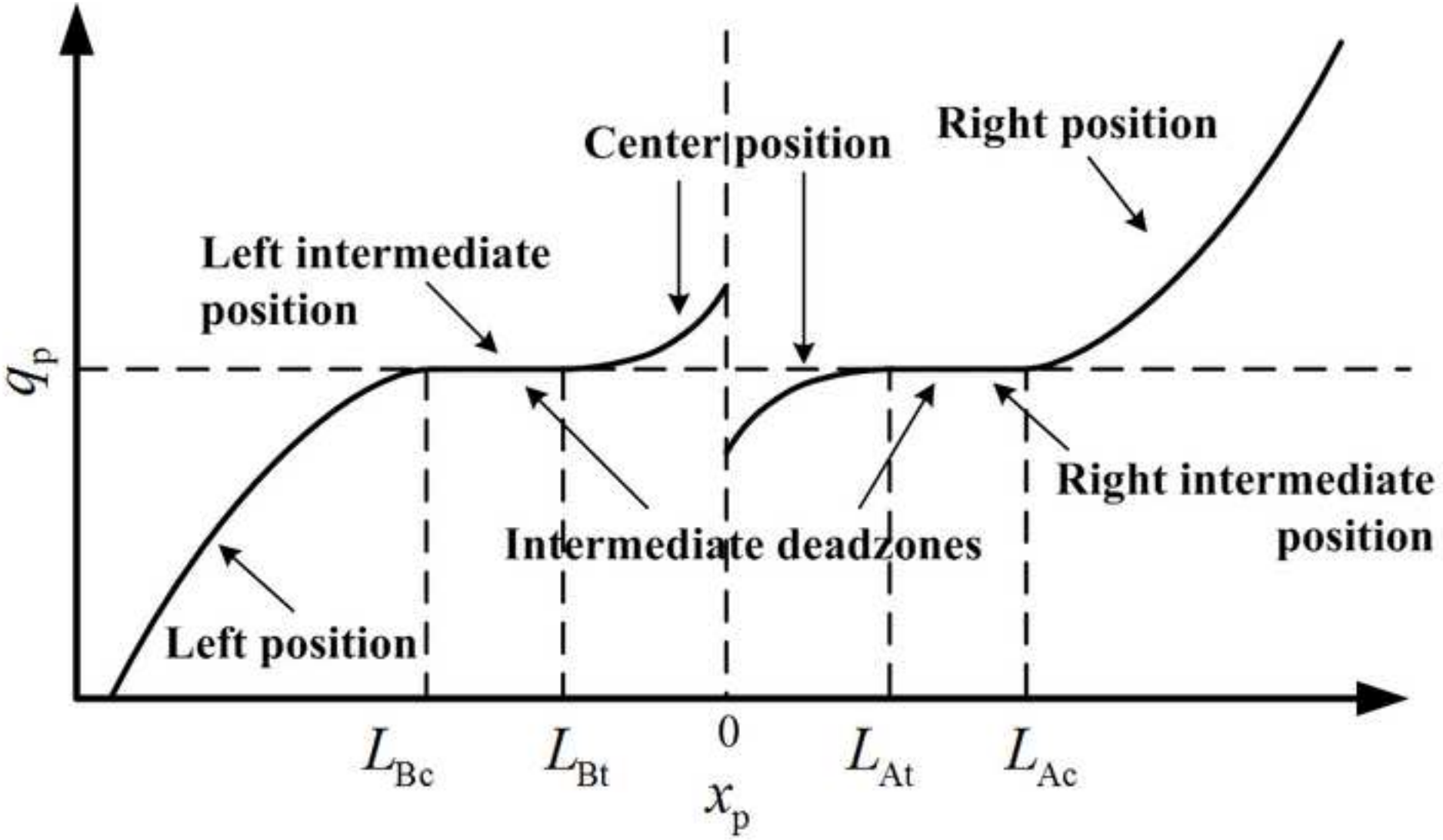

Figure 5

Click here to download high resolution image

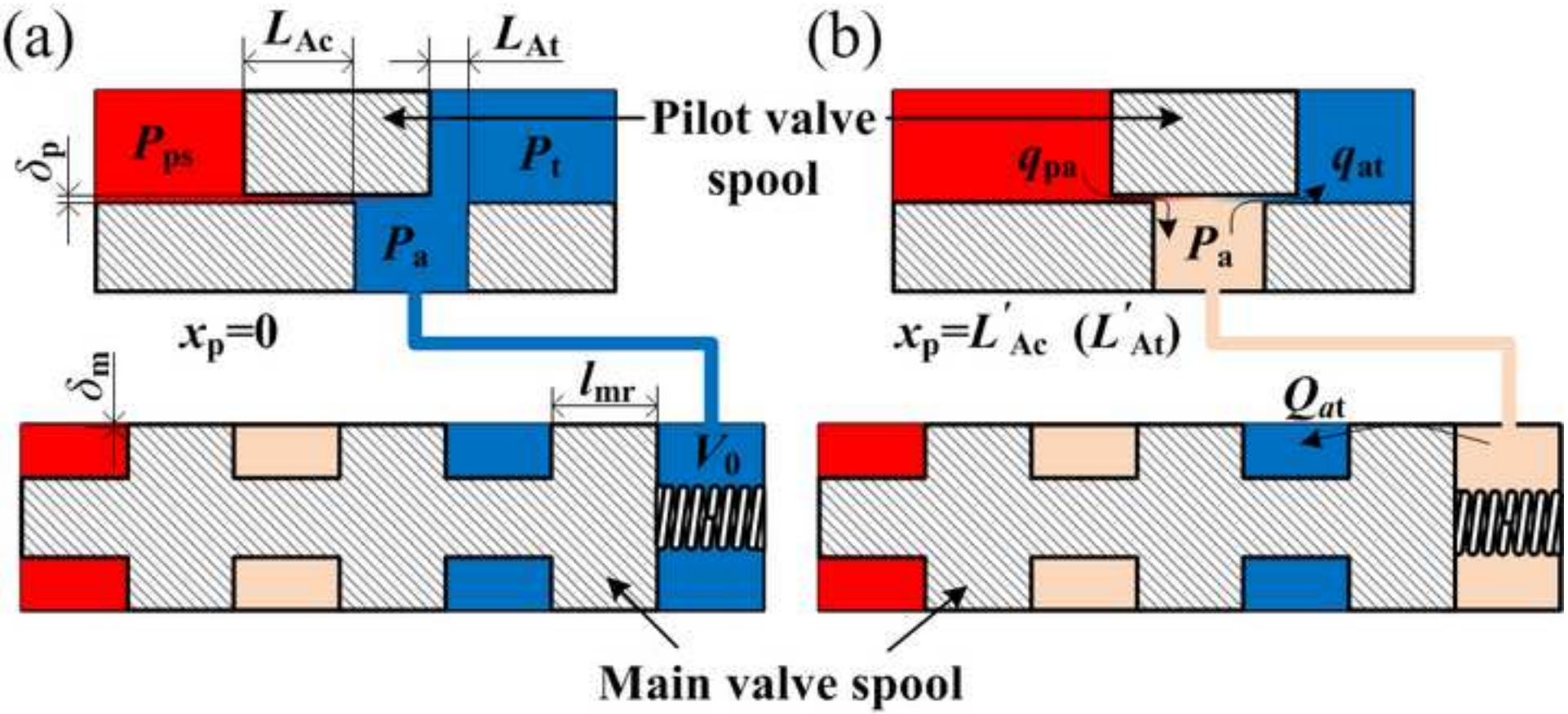

Figure 6

Click here to download high resolution image

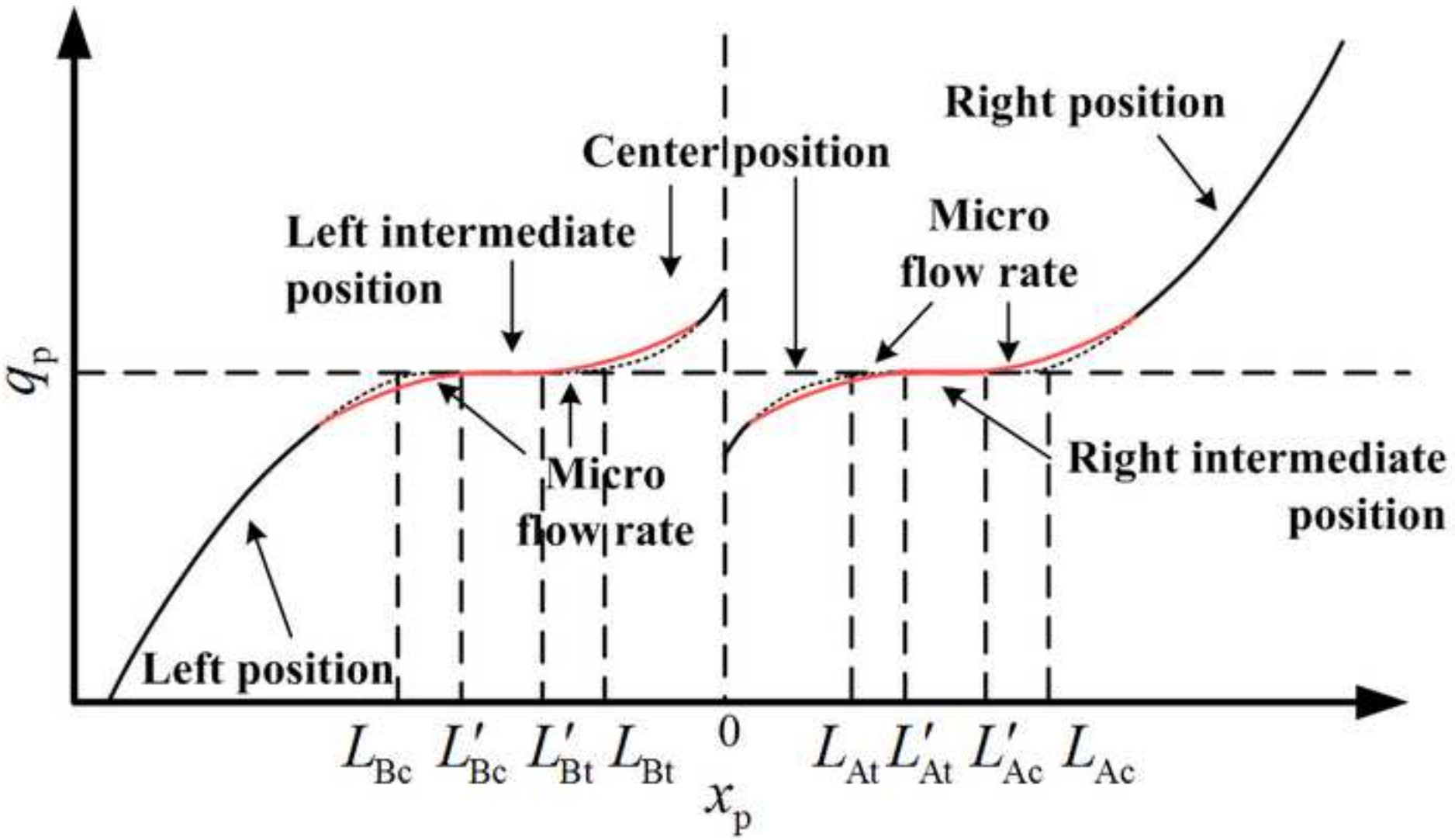

Figure 7

Click here to download high resolution image

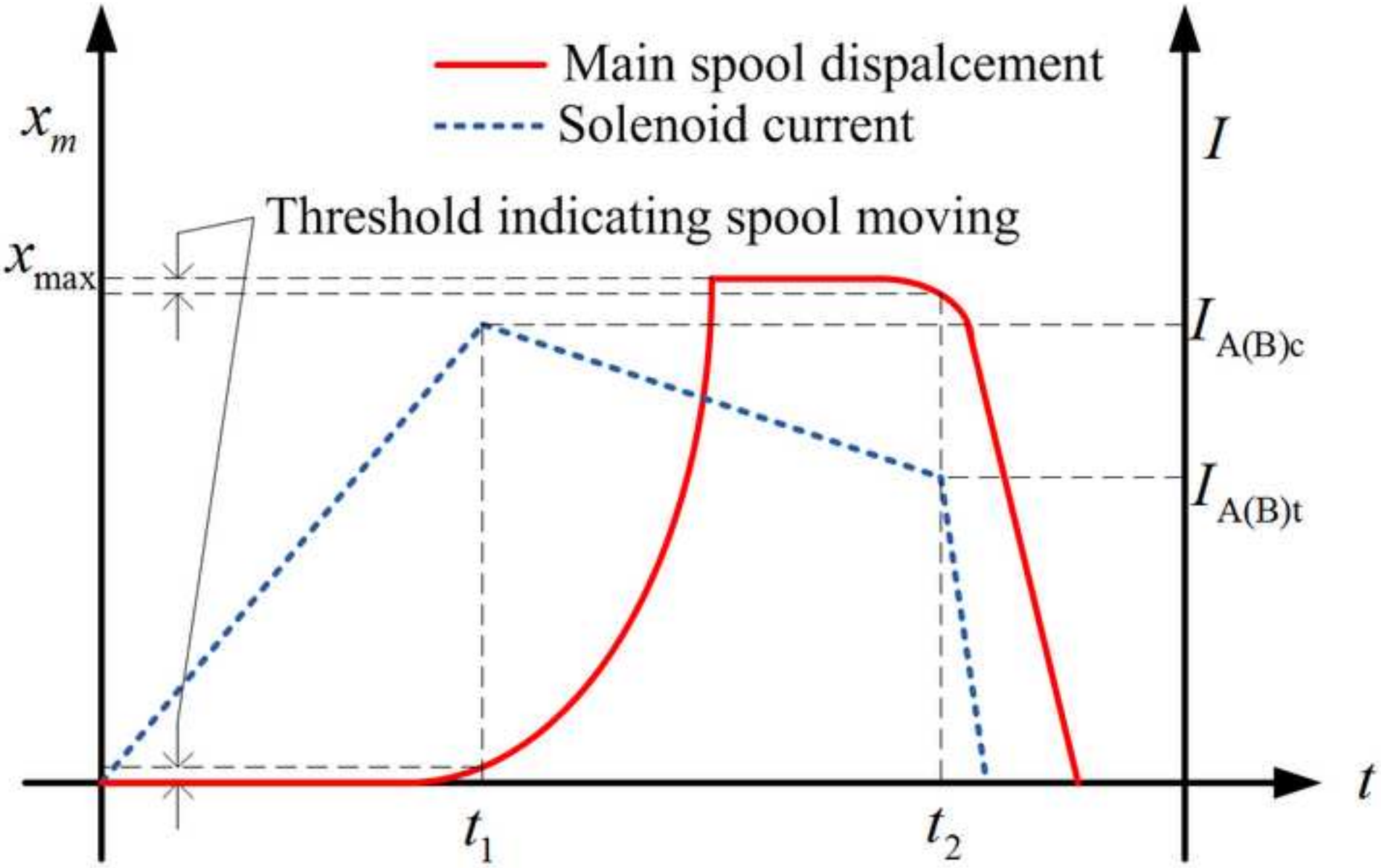

Figure 8

Click here to download high resolution image

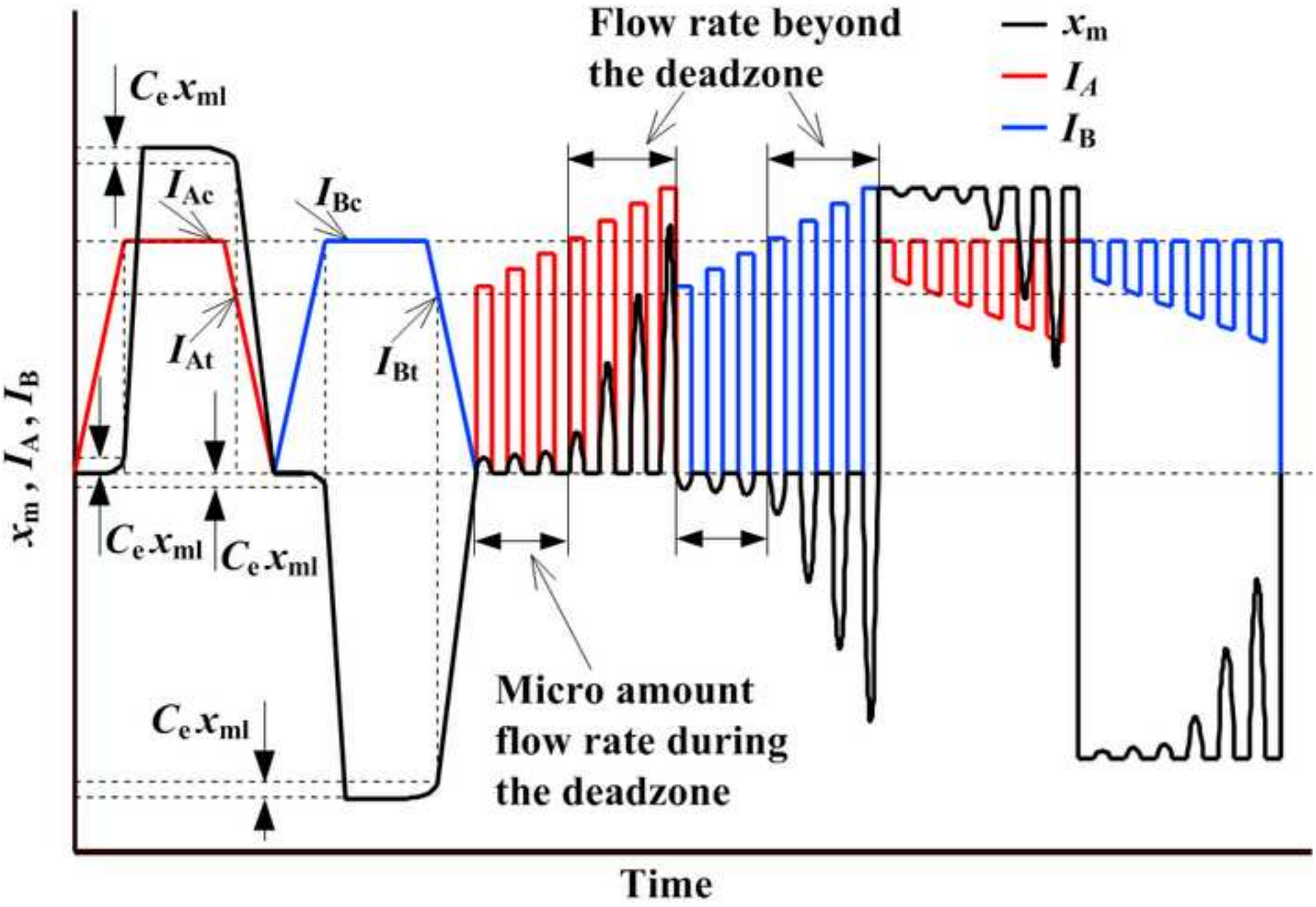

Figure 9

Click here to download high resolution image

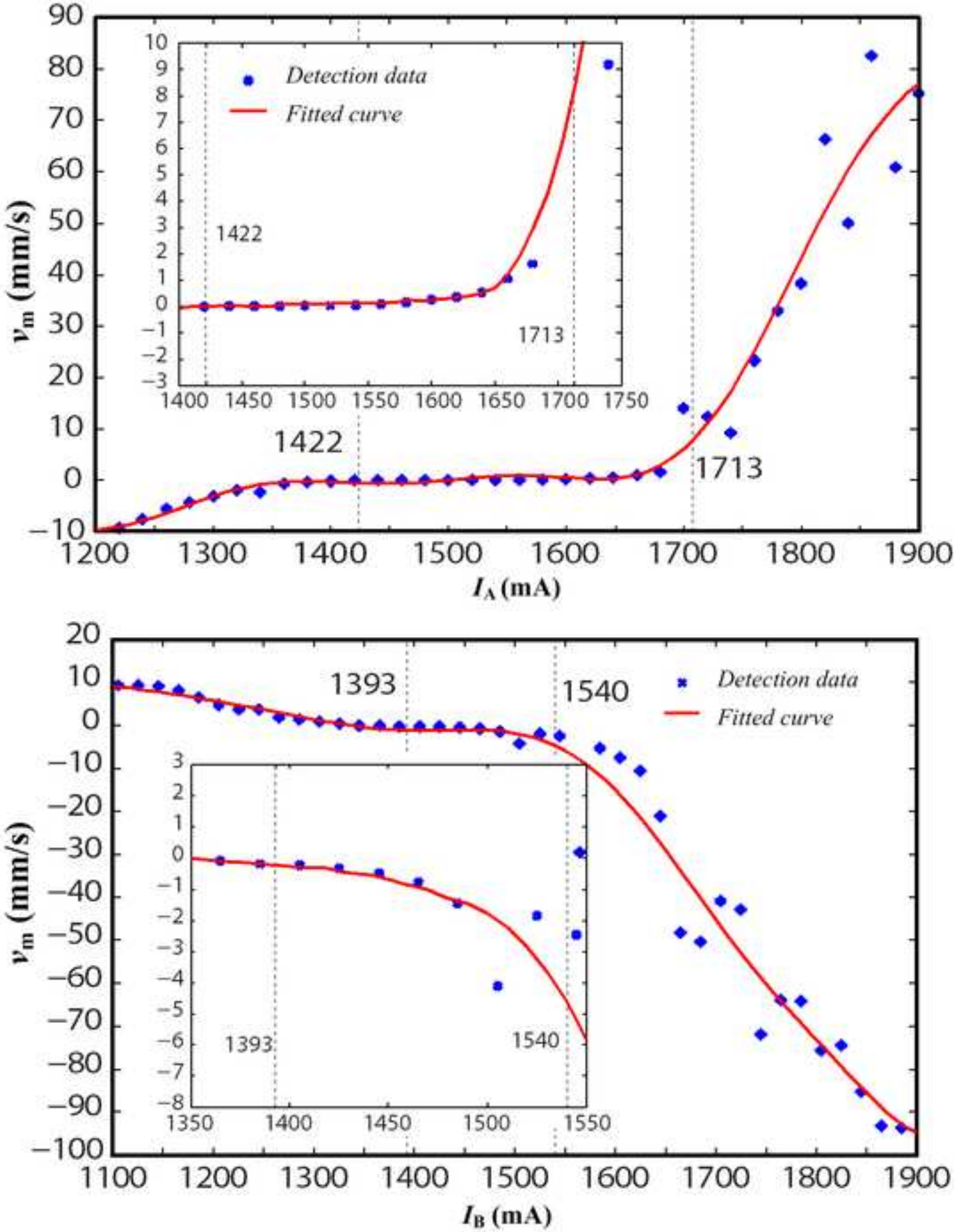

**Figure 10**

Click here to download high resolution image

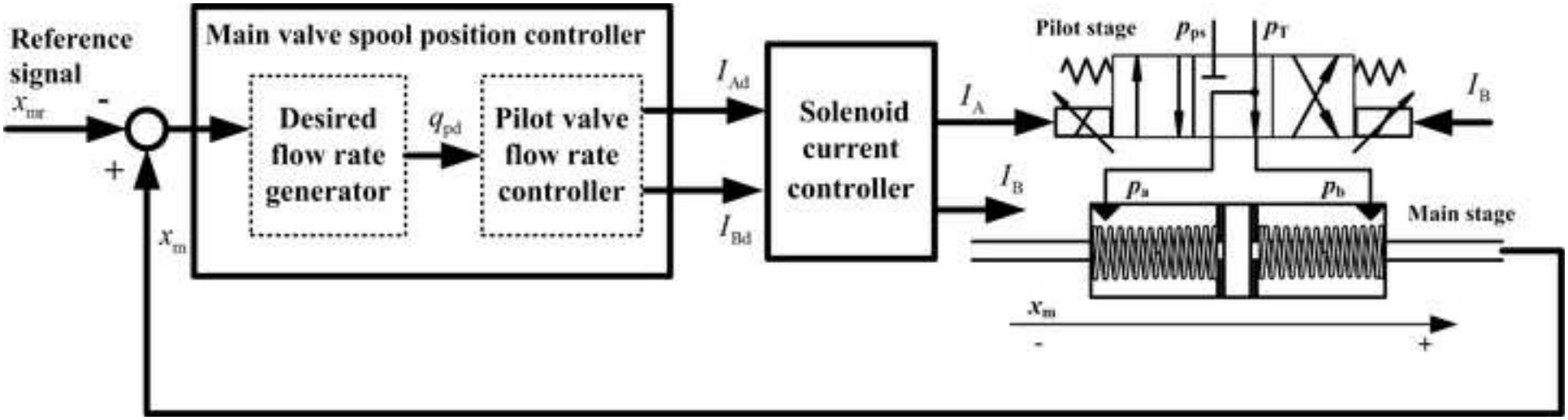

**Figure 11**

**Click here to download high resolution image**

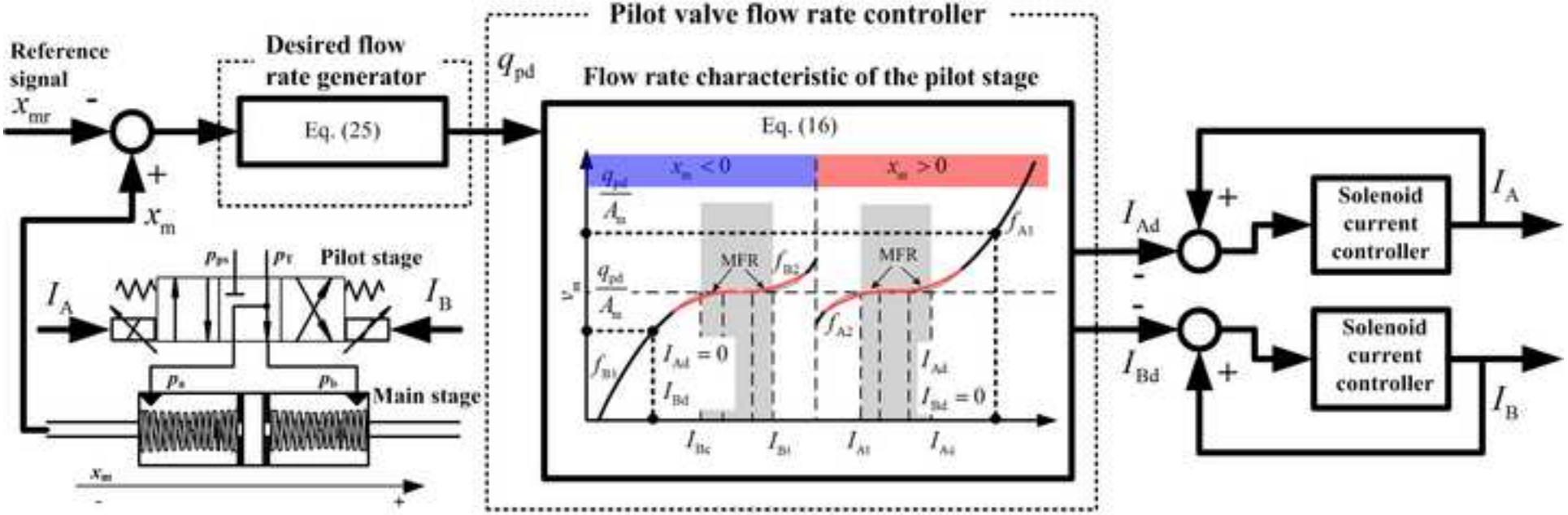

**Figure 12**

**Click here to download high resolution image**

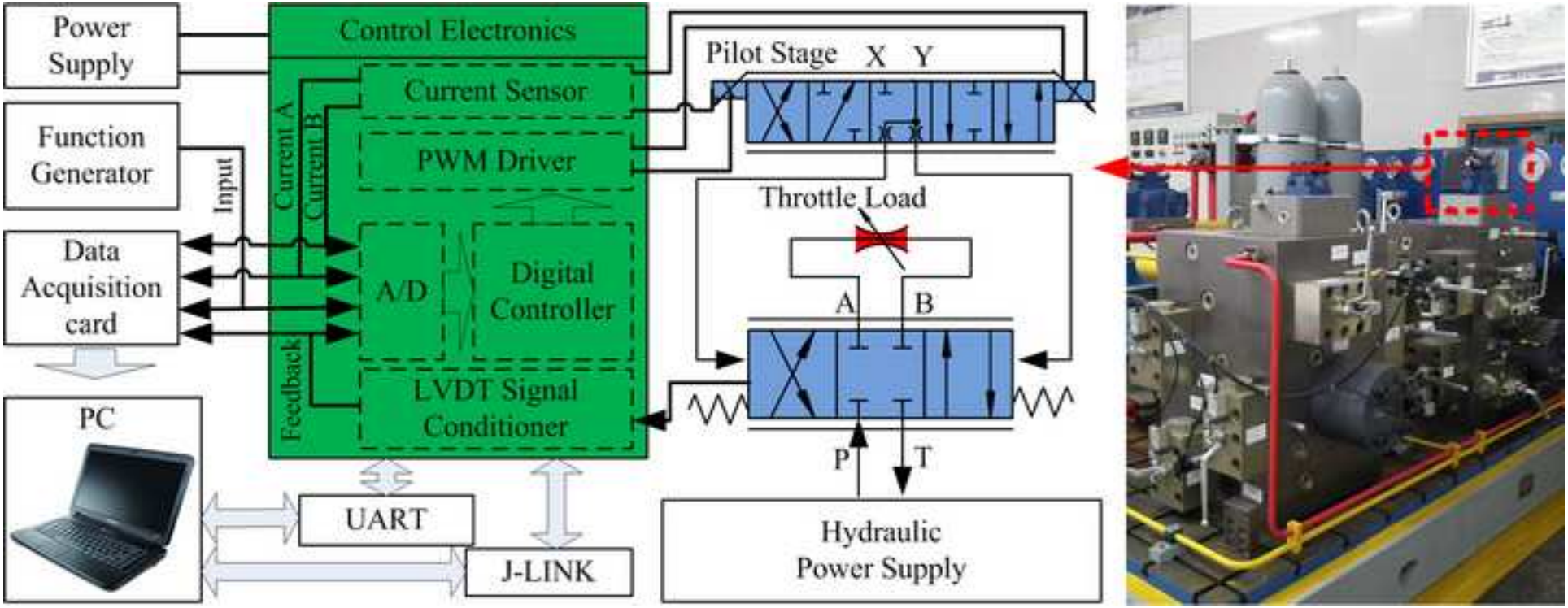

Figure 13

Click here to download high resolution image

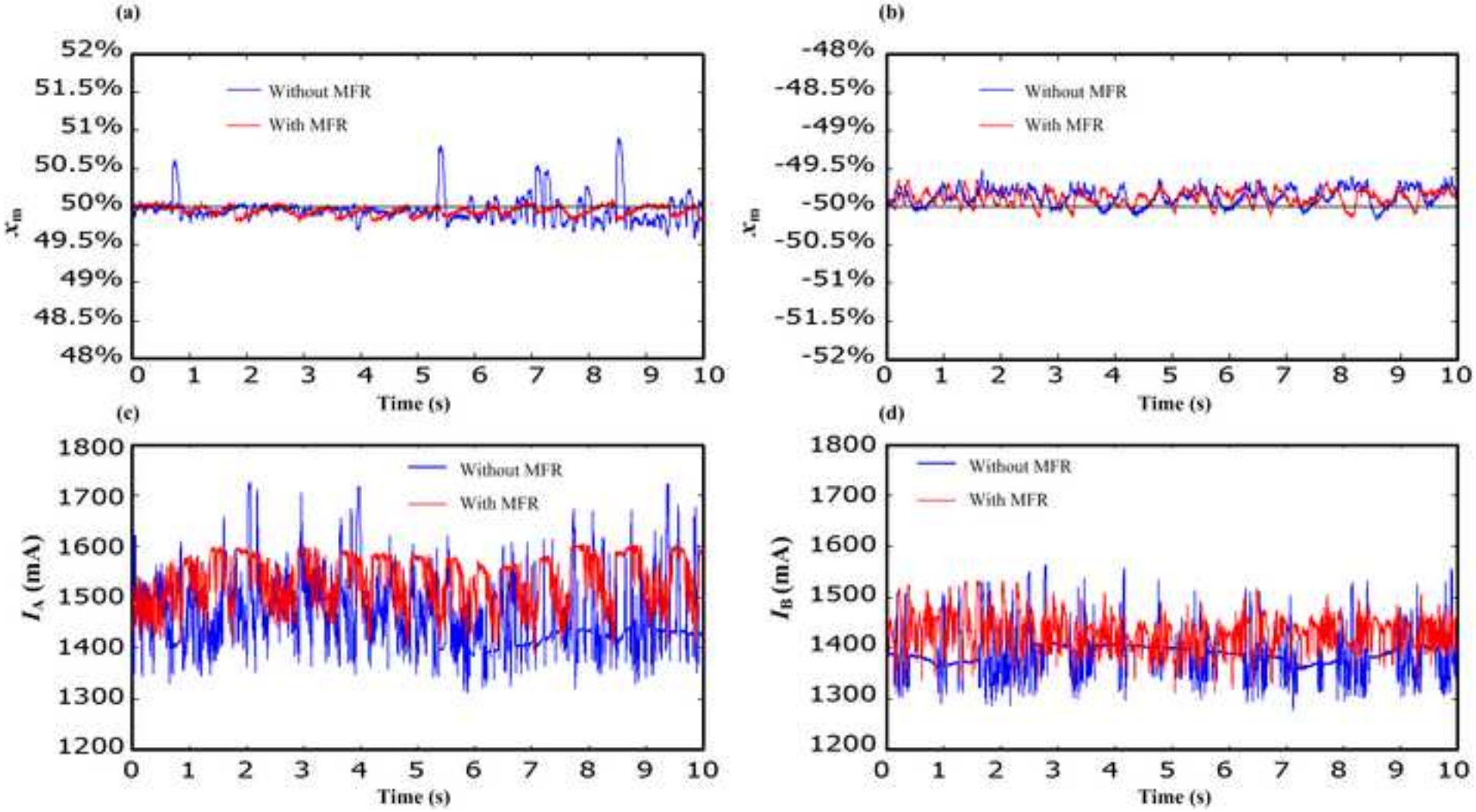

Figure 14

Click here to download high resolution image

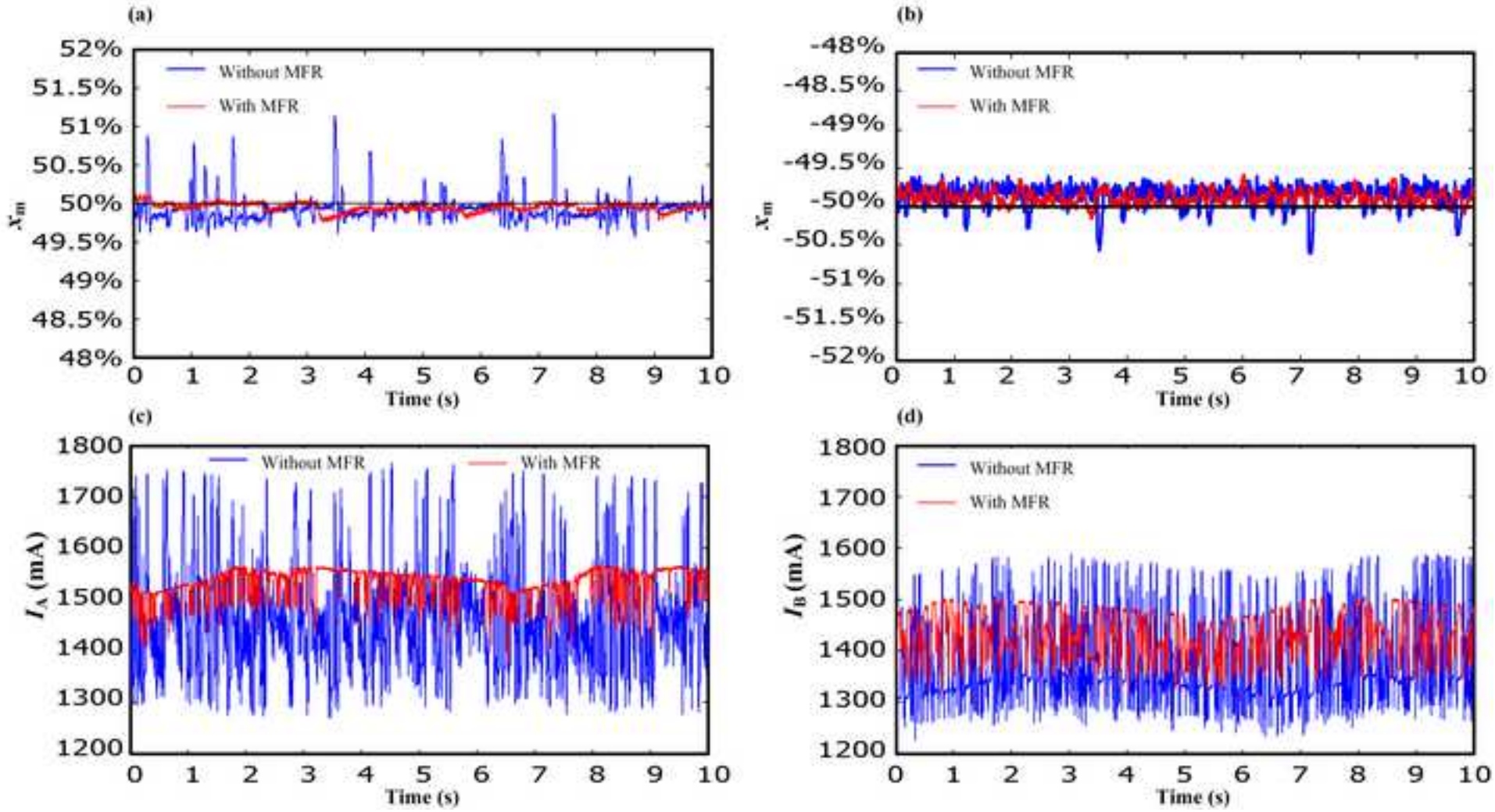

Figure 15

Click here to download high resolution image

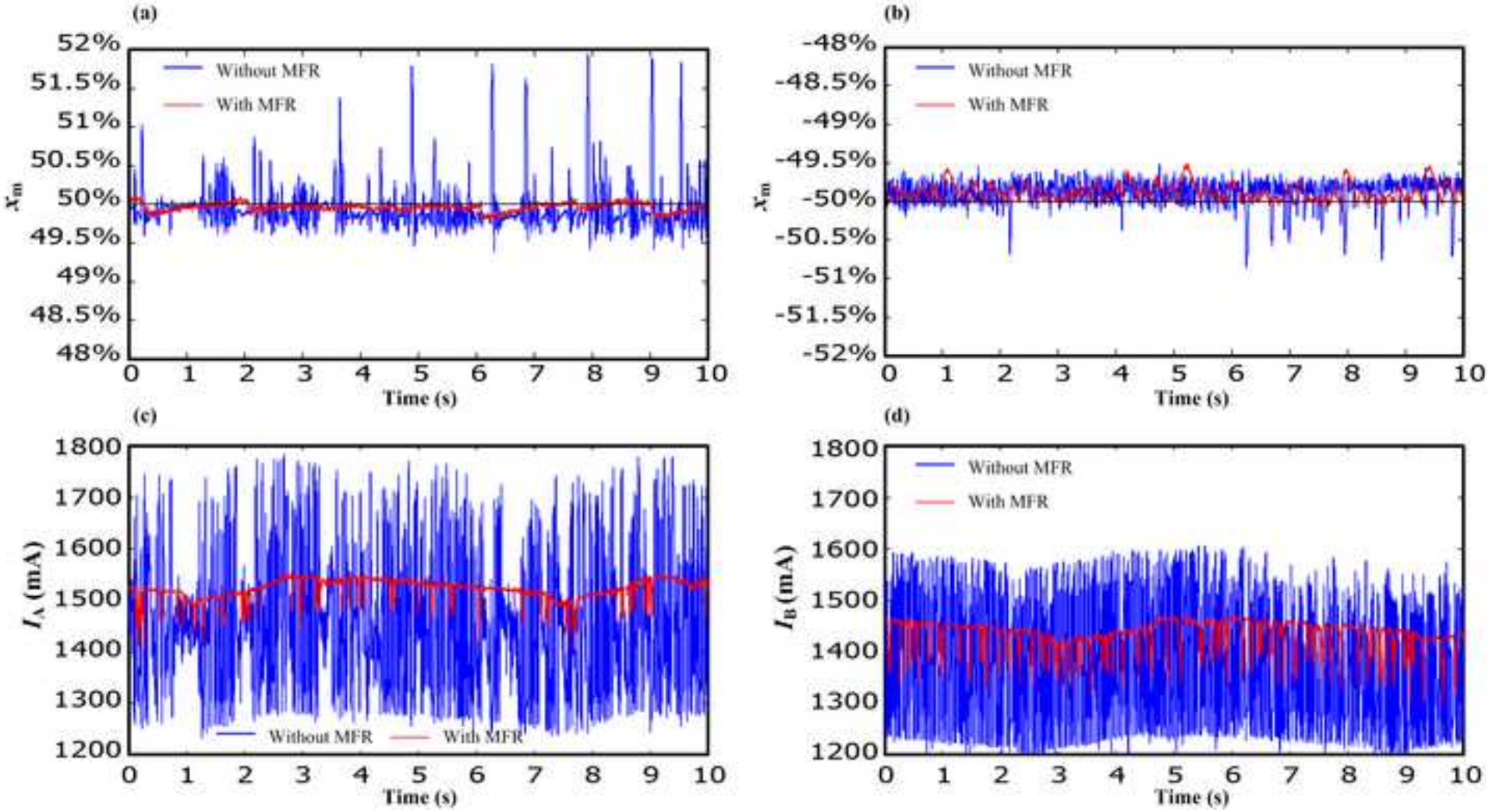

**Figure 16**

Click here to download high resolution image

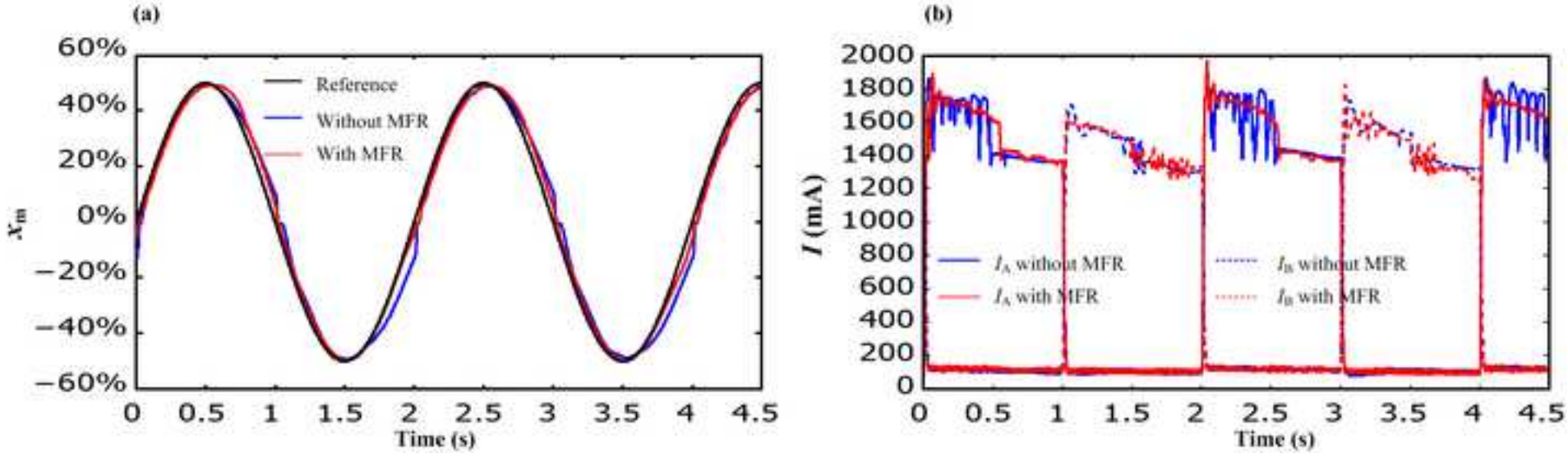

***Conflict of Interest**

**Declaration of interests**

☒ The authors declare that they have no known competing financial interests or personal relationships that could have appeared to influence the work reported in this paper.

☐The authors declare the following financial interests/personal relationships which may be considered as potential competing interests: